

Linear Analysis of PHIL Experiments & Partial Virtual DIM Interface Algorithm

- ▶ Harsha Ravindra
- ▶ Center for Advanced Power Systems,
Florida State University, Tallahassee



Outline

- Linear Analysis of Multi-Phase PHIL Experiments
- PV-DIM and its application



Motivation for Linear Analysis Framework

- PHIL experiment analysis is typically specific to case study and PHIL interface algorithm being used
- Most multi-phase PHIL experiments are conducted without proper assessment of
 - Stability
 - Accuracy
 - Sensitivity
- Advantages / Uses
 - Single framework that allows for probing of various IAs for an experiment
- Challenges
 - Properly represent the transfer functions needed within the linear analysis framework

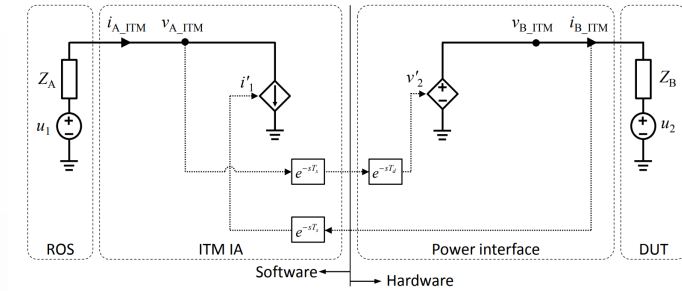


Fig. 3 PHIL system with ITM IA

ITM - IA

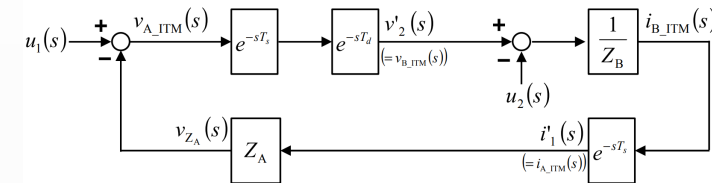


Fig. 4 Equivalent block diagram of the PHIL system with ITM IA

Same PHIL experiment analyzed differently due to two different IA used

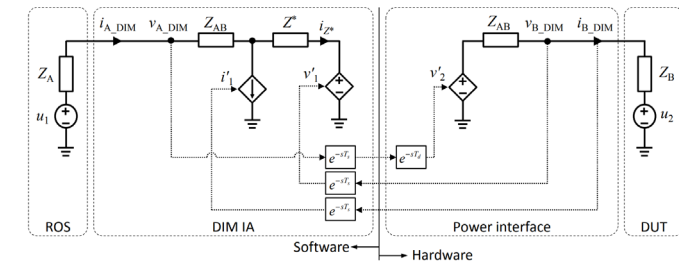


Fig. 5 PHIL system with DIM IA

DIM - IA

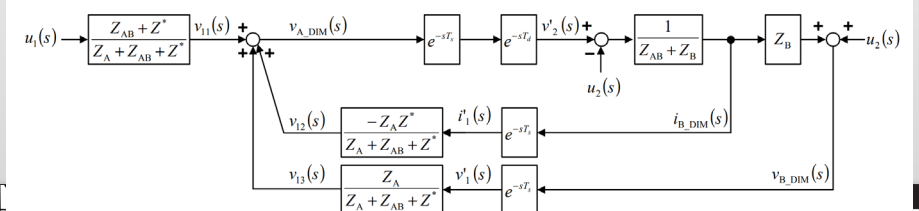
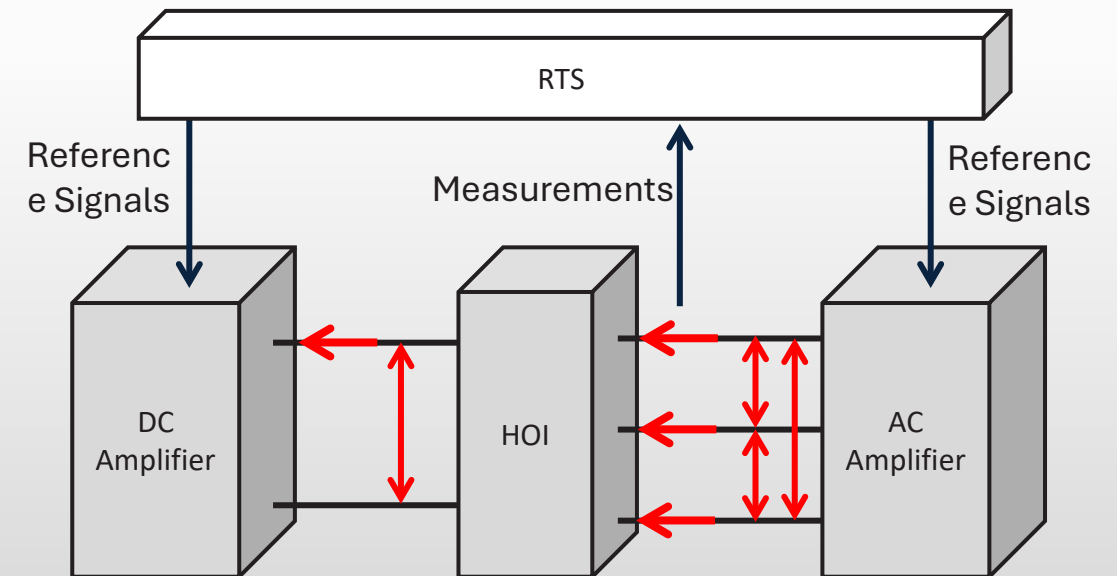
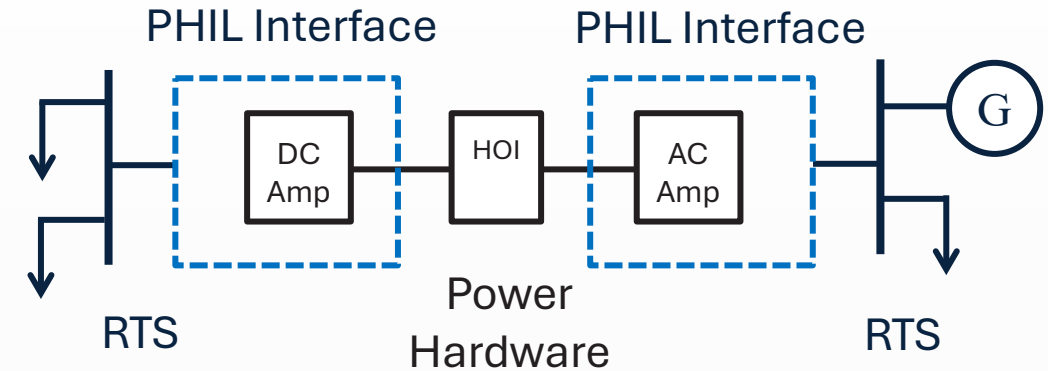


Fig. 6 Equivalent block diagram of the PHIL system with DIM IA

Power Hardware-in-the-Loop (PHIL) Simulation

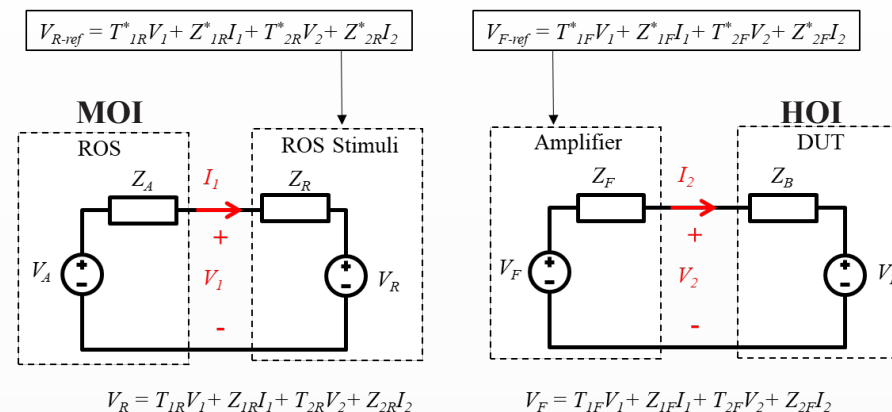
- Virtually interface power hardware of interest (HOI) to model of interest (MOI)
- Use power amplifiers and/or actuators in PHIL interface
- Advantages / Uses
 - Facilitates early integration testing
 - Flexibility to easily change surrounding system
 - Test extreme conditions in controlled laboratory environment
- Challenges
 - Delays in PHIL interface can adversely affect accuracy and stability



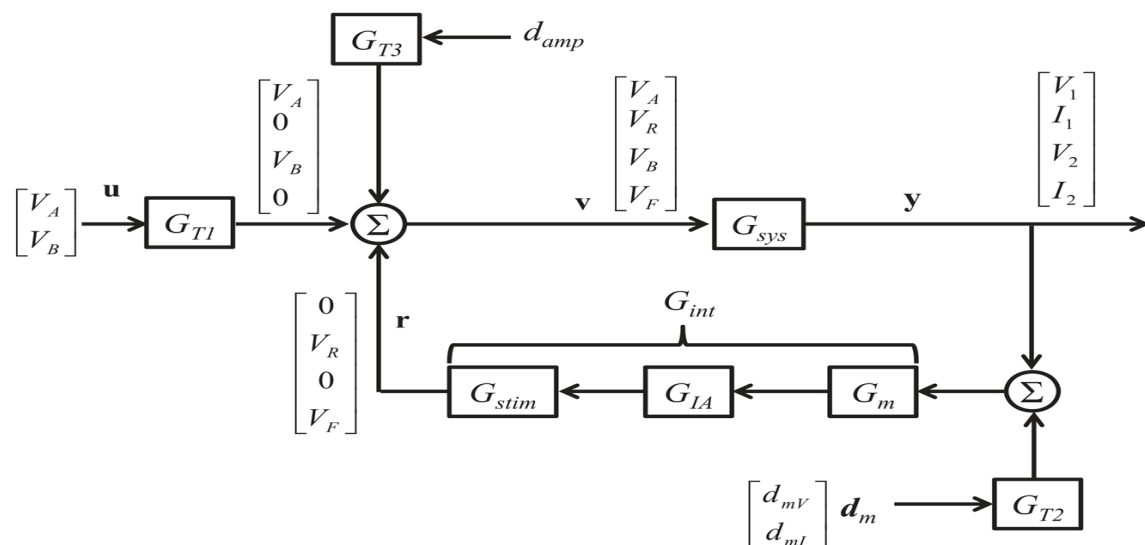


Linear Analysis Framework Using ELA for Single Phase PHIL System

- Extended Lawrence Architecture is applied as general framework for linear PHIL IAs
- Stimuli represented as Thevenin equivalent circuits
- Stimuli references formed from linear combination of observable quantities
- PHIL IA defined by 8 ideal “gains” and two Thevenin impedance characteristics (Z_R and Z_F)



Example PHIL Simulation Employing IA of ELA



G_{sys} – Mapping from inputs and stimuli to observable quantities

G_{int} – Represents PHIL interface

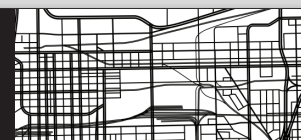
G_m – Effect of voltage and current sensors

G_{IA} – IA gains

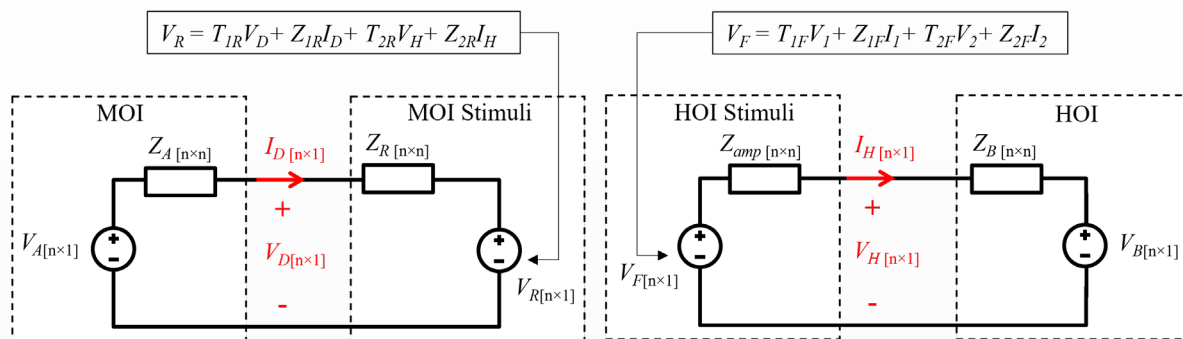
G_{stim} – Effects of amplification and stimulation injections

d_m – Noise at sensors measurements

d_{amp} – Disturbance introduced through amplifier



Linear Formulation for Multi-Phase PHIL Interfaces

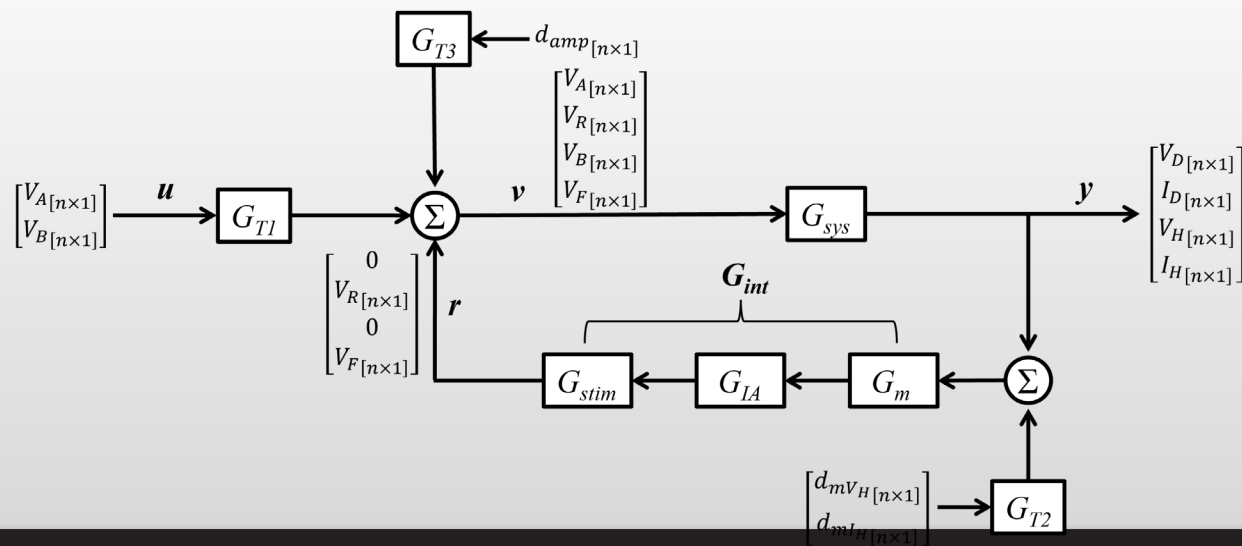


$$G_{T1} = \begin{bmatrix} \mathbf{I}_n & \mathbf{0}_n & \mathbf{0}_n & \mathbf{0}_n \\ \mathbf{0}_n & \mathbf{0}_n & \mathbf{I}_n & \mathbf{0}_n \end{bmatrix}^T \quad G_{T2} = \begin{bmatrix} \mathbf{0}_n & \mathbf{0}_n & \mathbf{I}_n & \mathbf{0}_n \\ \mathbf{0}_n & \mathbf{0}_n & \mathbf{0}_n & \mathbf{I}_n \end{bmatrix}^T$$

$$G_{sys} = \begin{bmatrix} (Z_A + Z_R)^{-1} Z_R & (Z_A + Z_R)^{-1} Z_A & \mathbf{0}_n & \mathbf{0}_n \\ (Z_A + Z_R)^{-1} & -(Z_A + Z_R)^{-1} & \mathbf{0}_n & \mathbf{0}_n \\ \mathbf{0}_n & \mathbf{0}_n & (Z_B + Z_F)^{-1} Z_F & (Z_B + Z_F)^{-1} Z_B \\ \mathbf{0}_n & \mathbf{0}_n & -(Z_B + Z_F)^{-1} & (Z_B + Z_F)^{-1} \end{bmatrix}$$

$$G_{IA} = \begin{bmatrix} \mathbf{0}_n & \mathbf{0}_n & \mathbf{0}_n & \mathbf{0}_n \\ T_{DR}^* & Z_{DR}^* & T_{HR}^* & Z_{HR}^* \\ \mathbf{0}_n & \mathbf{0}_n & \mathbf{0}_n & \mathbf{0}_n \\ T_{DF}^* & Z_{DF}^* & T_{HF}^* & Z_{HF}^* \end{bmatrix}$$

$$G_m = \begin{bmatrix} T_{mS} & \mathbf{0}_n & \mathbf{0}_n & \mathbf{0}_n \\ \mathbf{0}_n & T_{mS} & \mathbf{0}_n & \mathbf{0}_n \\ \mathbf{0}_n & \mathbf{0}_n & T_{mV} & \mathbf{0}_n \\ \mathbf{0}_n & \mathbf{0}_n & \mathbf{0}_n & T_{mI} \end{bmatrix}$$



$$G_{stim} = \begin{bmatrix} \mathbf{0}_n & \mathbf{0}_n & \mathbf{0}_n & \mathbf{0}_n \\ \mathbf{0}_n & T_{stim} & \mathbf{0}_n & \mathbf{0}_n \\ \mathbf{0}_n & \mathbf{0}_n & \mathbf{0}_n & \mathbf{0}_n \\ \mathbf{0}_n & \mathbf{0}_n & \mathbf{0}_n & T_{amp} \end{bmatrix}$$

Linear Formulation for Multi-Phase PHIL Interfaces

Matrix	Description	Matrix Size
\mathbf{u}	Input applied at terminals of ROS and DUT	$2n \times 1$
\mathbf{y}	Observable quantities at the terminals of ROS and DUT	$4n \times 1$
\mathbf{v}	Matrix of input and stimuli	$4n \times 1$
\mathbf{r}	Stimuli applied to ROS and DUT	$4n \times 1$
G_{T1}	Conditioning matrix for \mathbf{u}	$4n \times 2n$
G_{T2}	Conditioning matrix to include effects of d_m	$4n \times 2n$
G_{T3}	Conditioning matrix to include effects of d_{amp}	$4n \times n$
G_{sys}	Matrix facilitating mapping of inputs and stimuli to observable quantities	$4n \times 4n$
G_m	Effects of voltage and current sensors	$4n \times 4n$
G_{IA}	Ideal gains of interface algorithm	$4n \times 4n$
G_{stim}	Effects of amplification and injection stage	$4n \times 4n$
G_{int}	Matrix representing the entire PHIL interface ($G_m G_{IA} G_{stim}$)	$4n \times 4n$

Evaluation of Stability

$$G_{st} = -1 + \det(\mathbf{I}_{4n} - G_{sys} G_{int})$$

Evaluation of Accuracy

$$T_{u-y} = (\mathbf{I}_{4n} - G_{sys} G_{int})^{-1} G_{sys} G_{T1}$$

Evaluation of Sensitivity from measurements to observable quantities

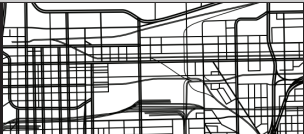
$$T_{dm-y} = (\mathbf{I}_{4n} - G_{sys} G_{int})^{-1} G_{sys} G_{int} G_{T2}$$

Evaluation of Sensitivity from amplifier disturbance to observable quantities

$$T_{damp-y} = (\mathbf{I}_{4n} - G_{sys} G_{int})^{-1} G_{sys} G_{T3}$$

ELA Gains of Existing PHIL IAs for Single-Phase PHIL Experiment

PHIL IA	T_{1R}^*	Z_{1R}^*	T_{2R}^*	Z_{2R}^*	T_{1F}^*	Z_{1F}^*	T_{2F}^*	Z_{2F}^*	Z_R	Z_F
ITM-VT	0	0	0	$-Z_R$	1	0	0	0	Z_R	Z_{amp}
ITM-IT	0	0	1	0	0	Z_{amp}	0	0	0	Z_{amp}
PCD-VT	0	0	1	0	1	0	0	0	Z_{AB}	$Z_{AB} + Z_{amp}$
PCD-IT	0	0	0	$-Z_{AB}$	0	$Z_{AB} // Z_{amp}$	0	0	Z_{AB}	$Z_{AB} // Z_{amp}$
DIM-VT	0	0	1	$-Z^*$	1	0	0	0	$Z^* + Z_{AB}$	$Z_{AB} + Z_{amp}$
DIM-IT	0	0	$\frac{Z_{AB}}{Z^* + Z_{AB}}$	$-Z^* // Z_{AB}$	0	$Z_{AB} // Z_{amp}$	0	0	$Z^* // Z_{AB}$	$Z_{AB} // Z_{amp}$
TLM	0	0	1	$-Z_{lk}$	1	Z_{lk}	0	0	Z_{lk}	$Z_{lk} + Z_{amp}$
AITM-VT	1	0	0	$-Z_C$	1	0	0	0	Z_C	Z_{amp}



Transfer Function from Input Voltage ($V_{A_d/q}$) to Observable Quantities ($V_{_d/q}$, $I_{_d/q}$)

- Symbolic expressions are not intuitive to analyze without simplifications
- Numerical analysis using symbolic expressions in FD are matched to TD simulations

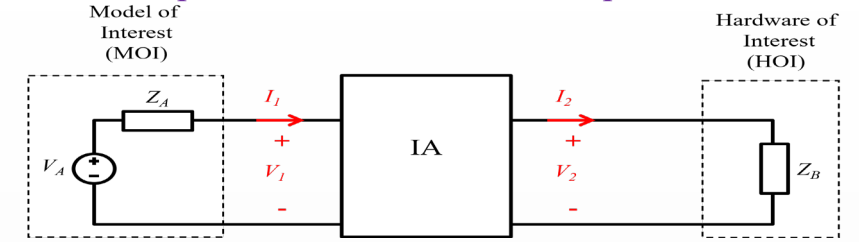
$$T_{VAd-V Dd} = \frac{(Z_R(Z_A Z_{Amp} + Z_A Z_B + Z_{Amp} Z_R + Z_B Z_R))}{((Z_A + Z_R)(Z_A Z_{Amp} + Z_A Z_B + Z_{Amp} Z_R + Z_B Z_R + T_{Amp} T_{mI} Z_A Z_R))}$$

$$T_{VAd-IDd} = \frac{1}{(Z_A + Z_R) + (T_{Amp} T_{mI} Z_R^2) / ((Z_A + Z_R)(Z_A Z_{Amp} + Z_A Z_B + Z_{Amp} Z_R + Z_B Z_R + T_{Amp} T_{mI} Z_A Z_R))}$$

$$T_{VAd-V Hd} = \frac{Z_R(T_{Amp} Z_A Z_B + T_{Amp} Z_B Z_R)}{((Z_A + Z_R)(Z_A Z_{Amp} + Z_A Z_B + Z_{Amp} Z_R + Z_B Z_R + T_{Amp} T_{mI} Z_A Z_R))}$$

$$T_{VAd-I Hd} = \frac{(T_{Amp} Z_R)}{(Z_A Z_{Amp} + Z_A Z_B + Z_{Amp} Z_R + Z_B Z_R + T_{Amp} T_{mI} Z_A Z_R)}$$

PHIL Implementation of the Ideal Experiment



- Resistive-Inductive DIM-VT Stability Analysis

$$G_{st} = \frac{Num}{Den}$$

$$\begin{aligned} Num = & Z_{Ampxy} (Z_{Bxy} + Z_{Byx}) (Z_A^2 + Z_{Ampxy} Z_{Bxy} + Z_A^2 + Z_{Ampxy} Z_{Byx} \\ & - Z_{Amp}^2 Z_{Axy} Z_{Byx} + Z_{Amp}^2 Z_{Ayx} Z_{Bxy} + Z_{Ampxy} Z_{Axy} Z_{Bxy}^2 + Z_{Ampxy} Z_{Ayx} Z_{Bxy}^2 \\ & - Z_{Ampxy}^2 Z_{Axy} Z_{Byx} + Z_{Ampxy}^2 Z_{Ayx} Z_{Bxy} - Z_{Axy} Z_B^2 Z_{Byx} + Z_{Ayx} Z_B^2 Z_{Bxy} \\ & + Z_{Axy} Z_{Bxy} Z_{Bxy}^2 - Z_{Ayx} Z_{Bxy}^2 Z_{Byx} - Z_{Ampxy} Z_{Axy} Z_{Ayx} Z_{Bxy} \\ & - Z_{Ampxy} Z_{Axy} Z_{Ayx} Z_{Byx} - 2Z_{Amp} Z_{Axy} Z_B Z_{Byx} + 2Z_{Amp} Z_{Ayx} Z_B Z_{Bxy} \\ & - Z_{Ampxy} Z_{Axy} Z_{Bxy} Z_{Byx} - Z_{Ampxy} Z_{Ayx} Z_{Bxy} Z_{Byx}) \end{aligned}$$

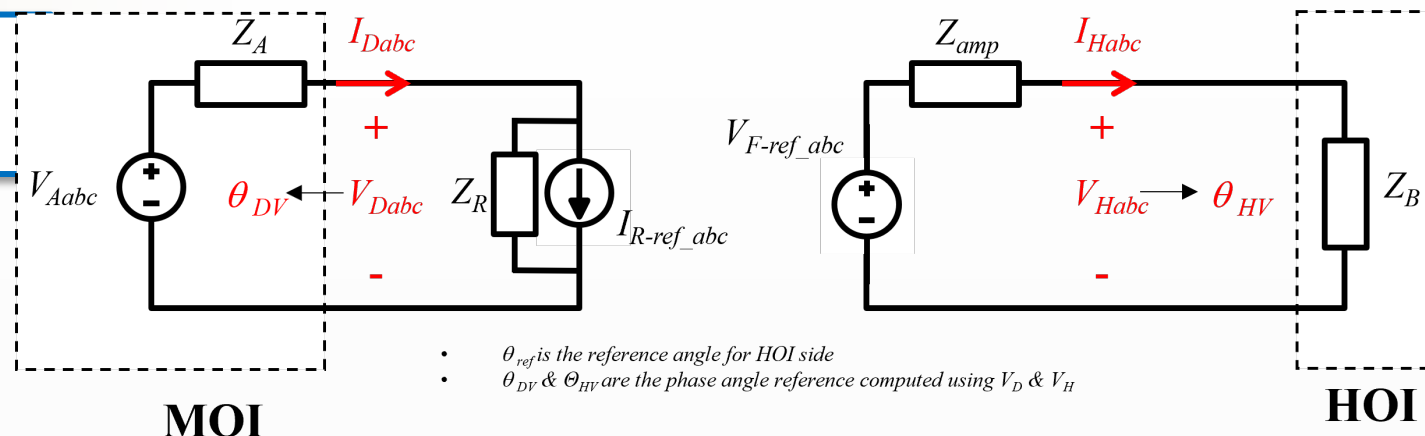
$$\begin{aligned} Den = & (2Z_{Amp} Z_B + Z_{Ampxy} Z_{Bxy} - Z_{Ampxy} Z_{Byx} - Z_{Bxy} Z_{Byx} + Z_{Amp}^2 \\ & + Z_B^2)^2 (-Z_A^2 - 2Z_A Z_B - Z_B^2 + Z_{Axy} Z_{Ayx} - Z_{Axy} Z_{Byx} + Z_{Ayx} Z_{Bxy} \\ & + Z_{Bxy} Z_{Byx}) \end{aligned}$$



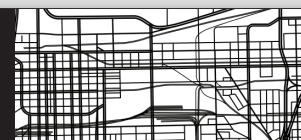
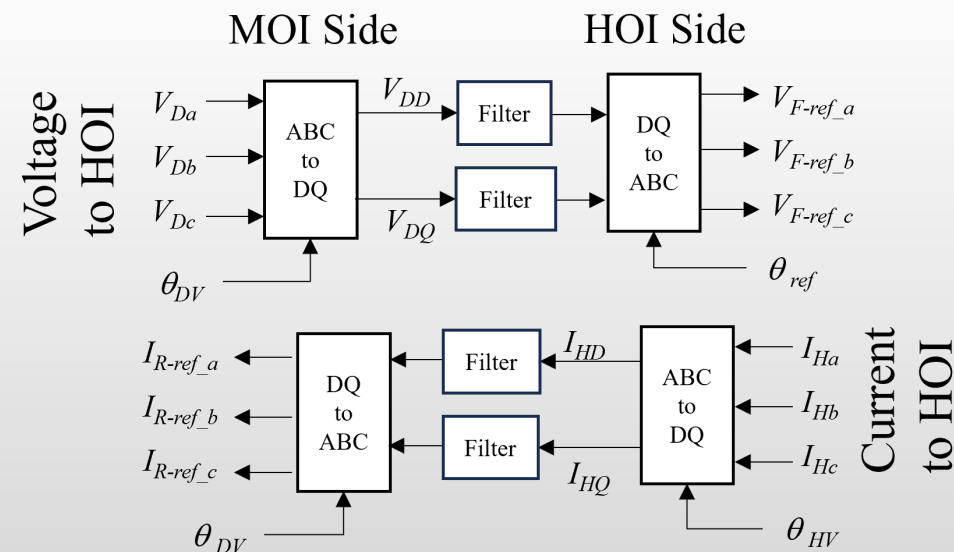
Example Application for System Using DQ-Frame PHIL ITM IA

- Frequency domain analysis conducted using Matlab
- Time-domain analysis conducted using RTDS

Symbol	Description	Default Value
f_{base}	Base frequency of the system	60 Hz
R_A	Source resistance	0.01 pu
X_A	Source reactance	0.05 pu
R_B	Load resistance	1 pu
X_B	Load reactance	0.75 pu
R_{amp}	Amplifier resistance	0.001 pu
X_{amp}	Amplifier reactance	0.005 pu
R_R	MOI stimulus resistance	10000 pu
X_R	MOI stimulus inductance	0 pu
f_{c-amp}	Pole frequency for filter representing the amplifier dynamics	1 kHz
f_{c-mI}	Pole frequency for filter representing current measurement characteristics	100 kHz
f_{c-mV}	Pole frequency for filter representing voltage measurement characteristics	100 kHz
T_{d-amp}	Amplifier time delay	150 μ s
T_{d-mI}	Time delay for measurement of currents at HOI	50 μ s
T_{d-mS}	Time delay for measurement of currents and voltages at MOI	50 μ s
T_{d-mV}	Time delay for measurement of voltages at HOI	50 μ s
T_{d-stim}	Time delay associated with application of voltage and current injections at simulated MOI	50 μ s

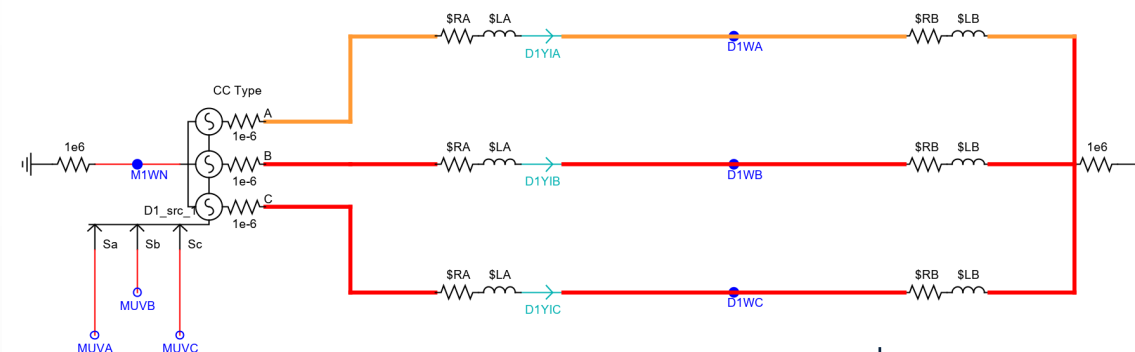


'DQ' transformation-based IA implementation

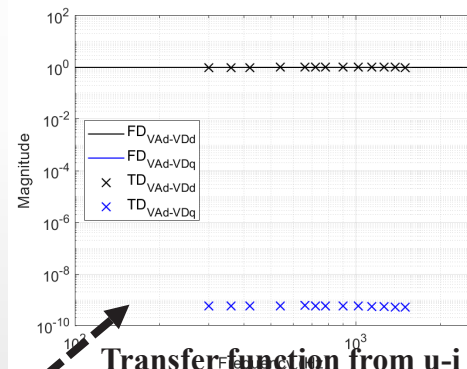
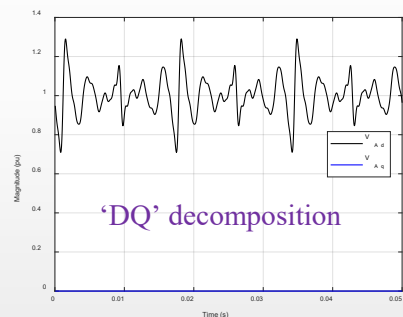




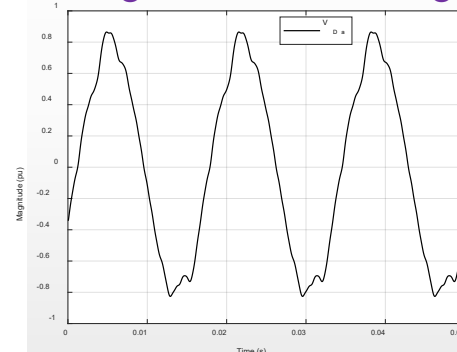
Time-Domain PHIL IA Implementation



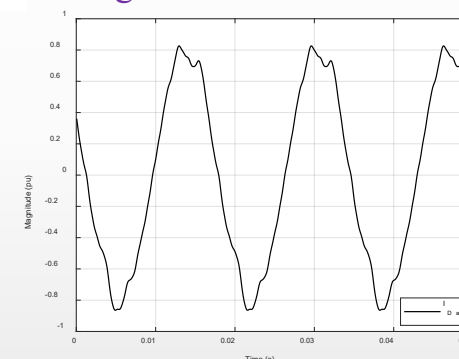
Ideal Experiment



Digital/Hardware Voltage



Digital/Hardware Current



Transfer function from u-i

ABC to DQ

ABC to DQ

Ratio

'D' Component Frequency Spectrum

'D' Component Frequency Spectrum

FFT

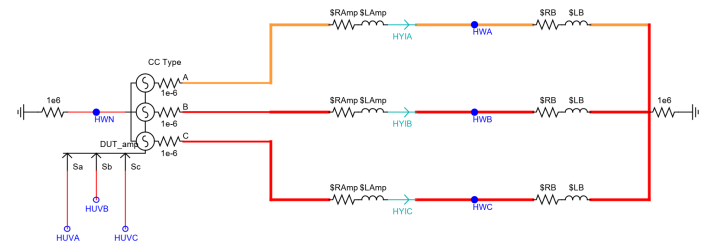
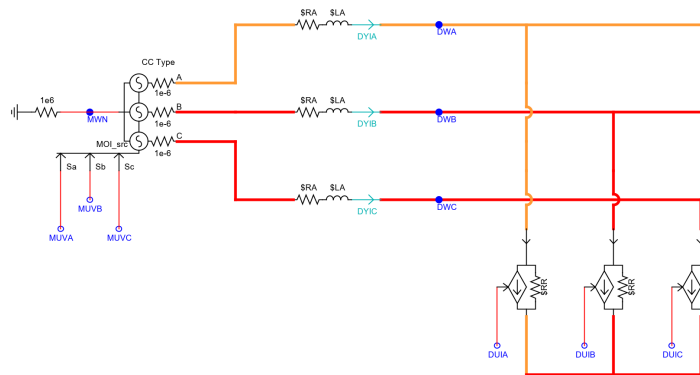
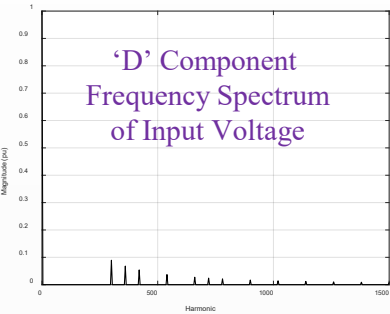
'DQ' decomposition

'DQ' decomposition

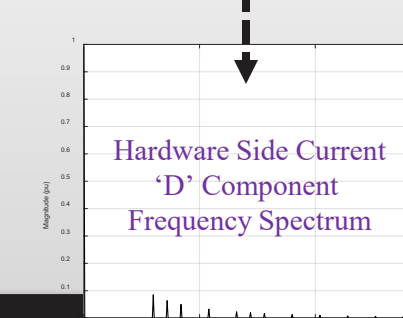
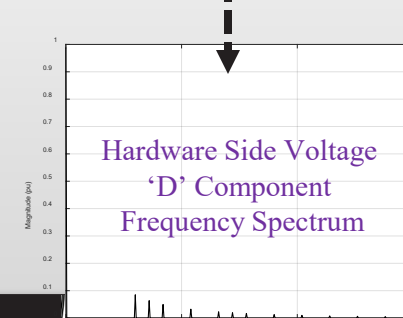
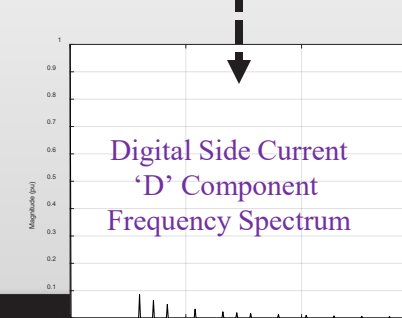
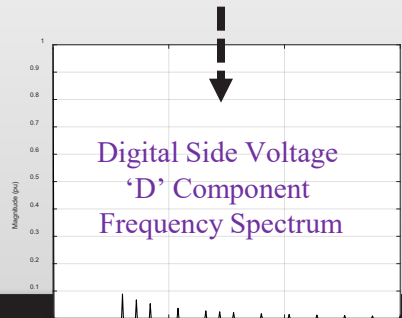
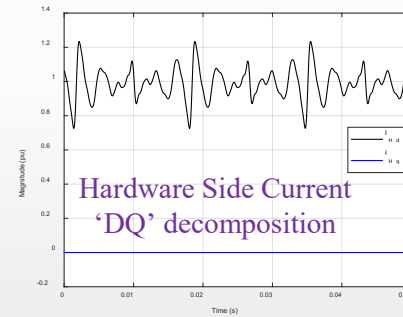
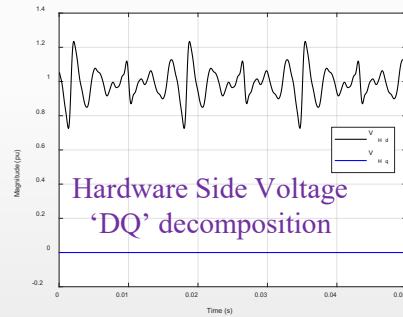
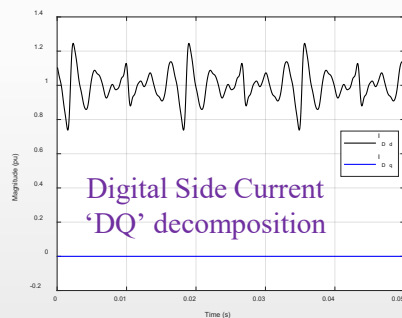
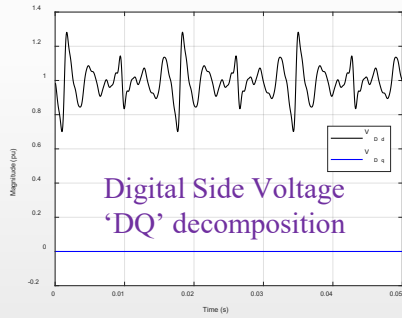
FFT

'D' Component Frequency Spectrum

Time-Domain PHIL IA Implementation on RTDS



ITM-VT Implementation of
Ideal Experiment



Evaluation of Stability

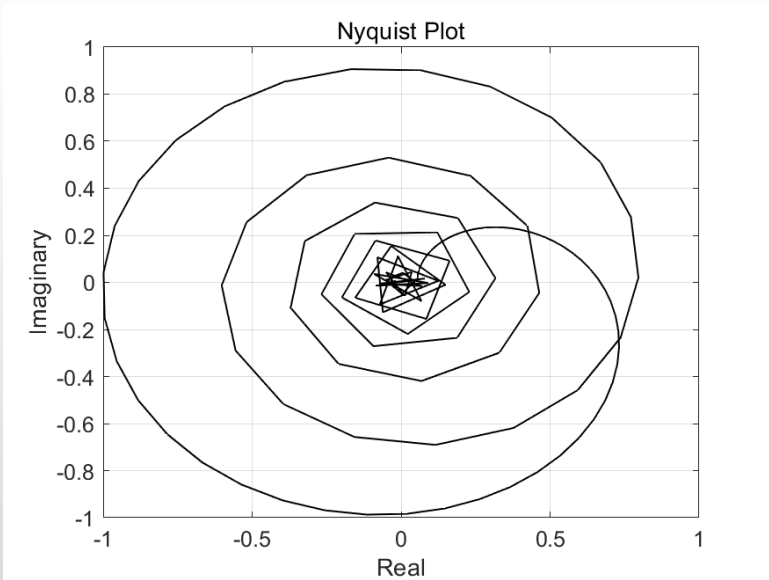
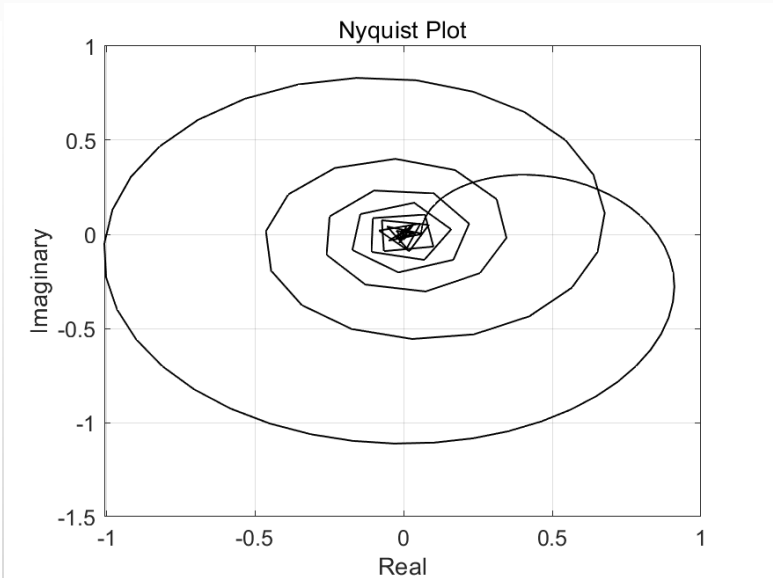
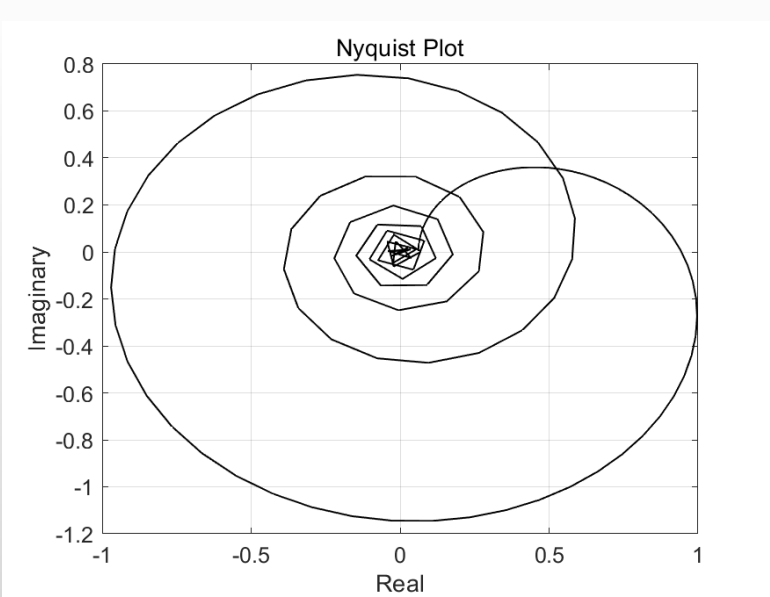
$\frac{Z_A}{Z_B}$ Ratio for Benchmark System to Reach Instability

Stability criteria with following simplifications

- All actuation measurement delays represented as T_d
- Within the controllable bandwidth, $Z_{Amp} = 0$

$$G_{st} = -T_d^3 \left(\frac{Z_A^2 T_d^3 + Z_{Adq}^2 T_d^3 + 2Z_A Z_B + 2Z_{Adq} Z_{Bdq}}{(Z_{Bdq}^2 + Z_B)^2} \right)$$

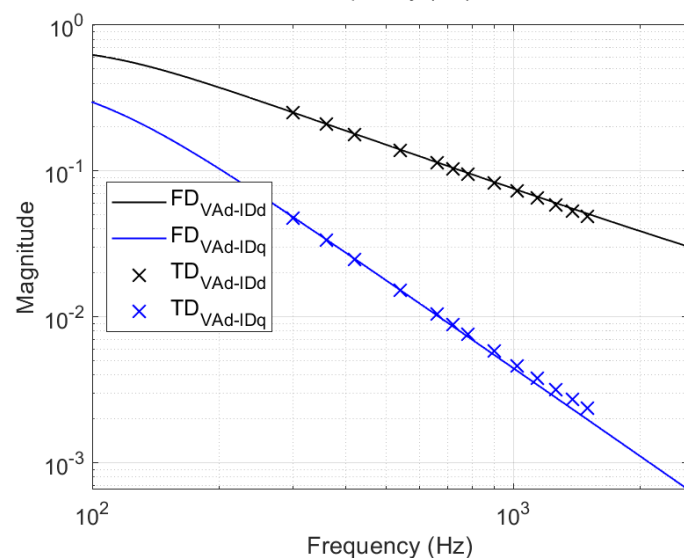
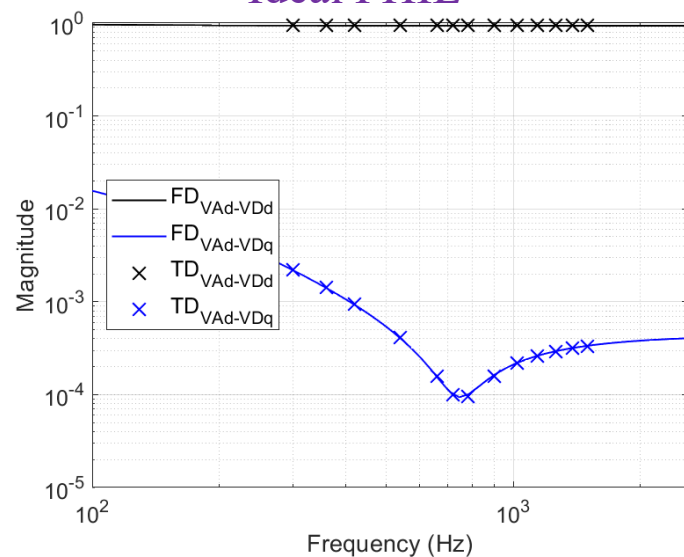
$T_{dAmp} (\mu s)$	Freq. Domain	Time-domain
150	0.31	0.31
250	0.29	0.29
300	0.28	0.28
500	0.27	0.27



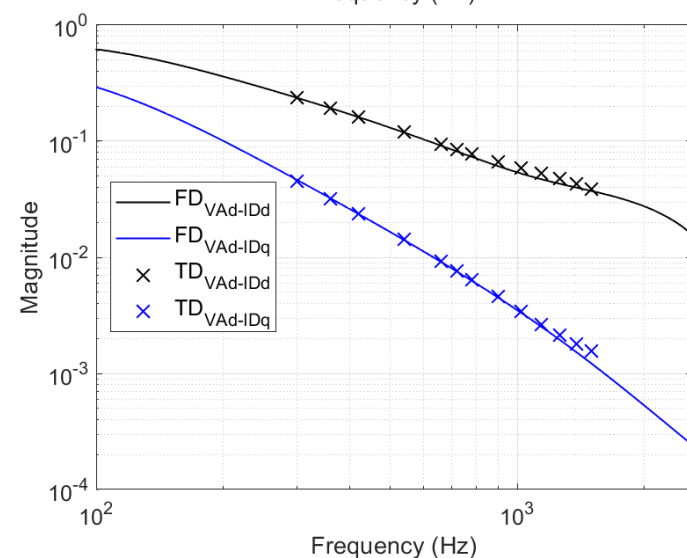
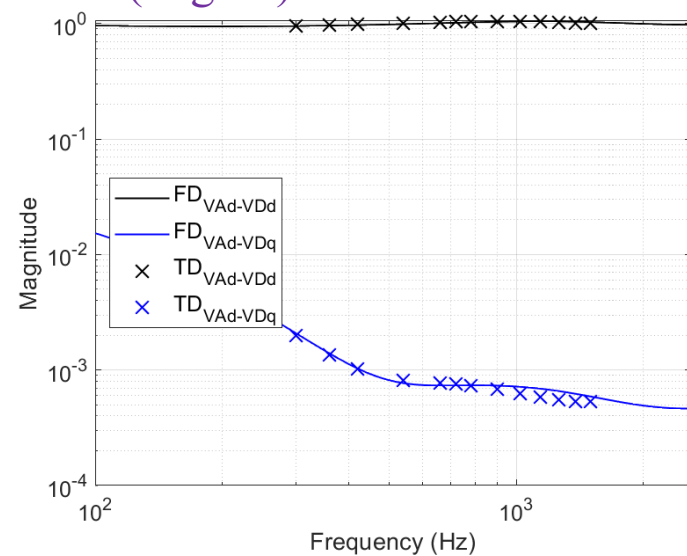


Evaluation of Accuracy

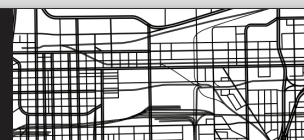
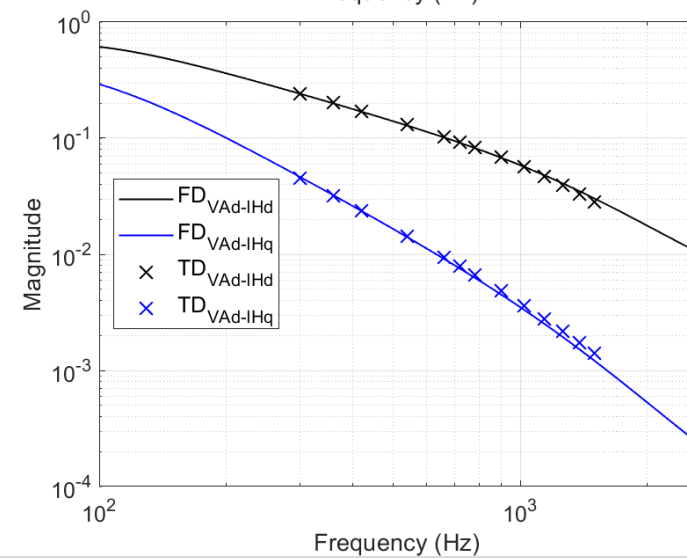
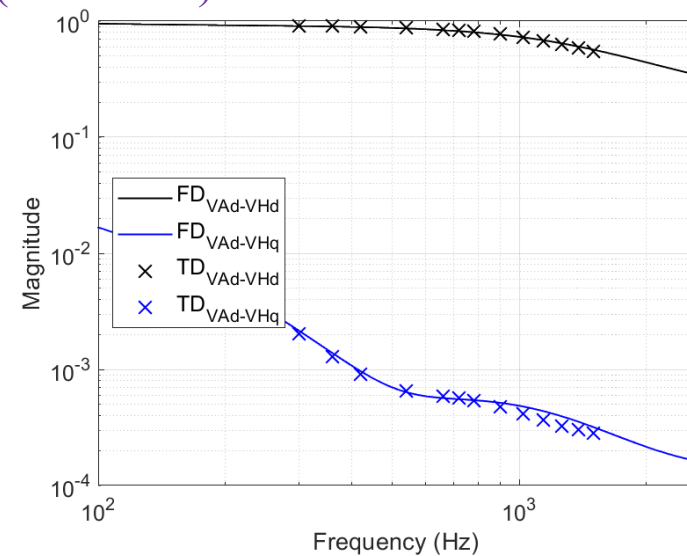
Ideal PHIL



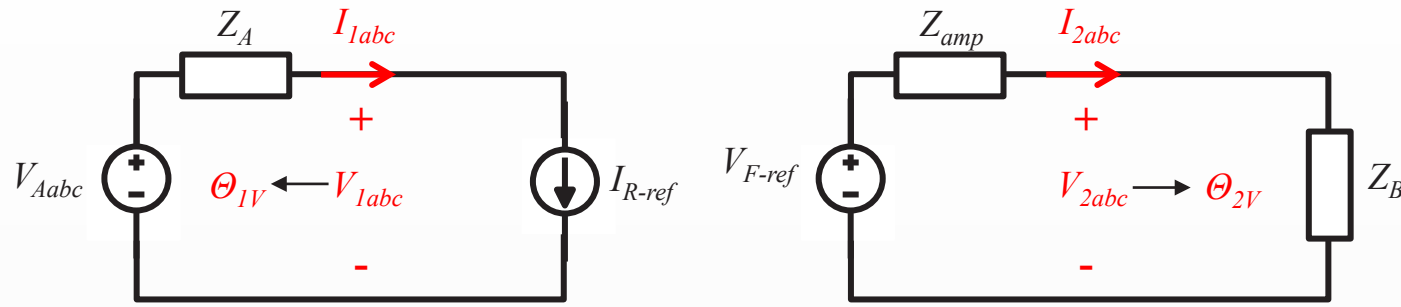
IA MOI (Digital) Side



IA HOI (Hardware) Side

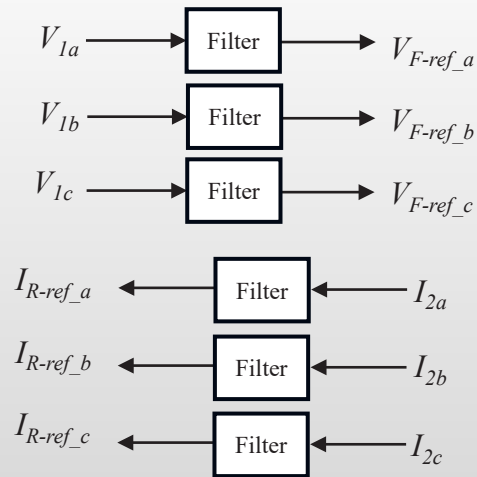


Phase Angle Accuracy Evaluation



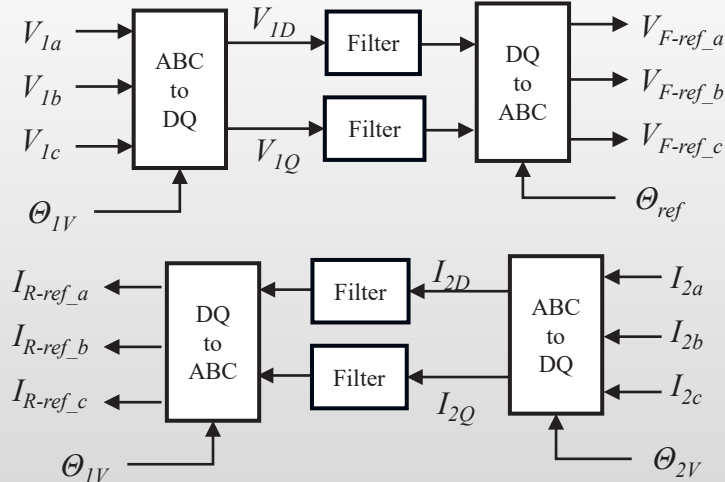
ITM-VT PHIL Experiment

'ABC' Frame Implementation

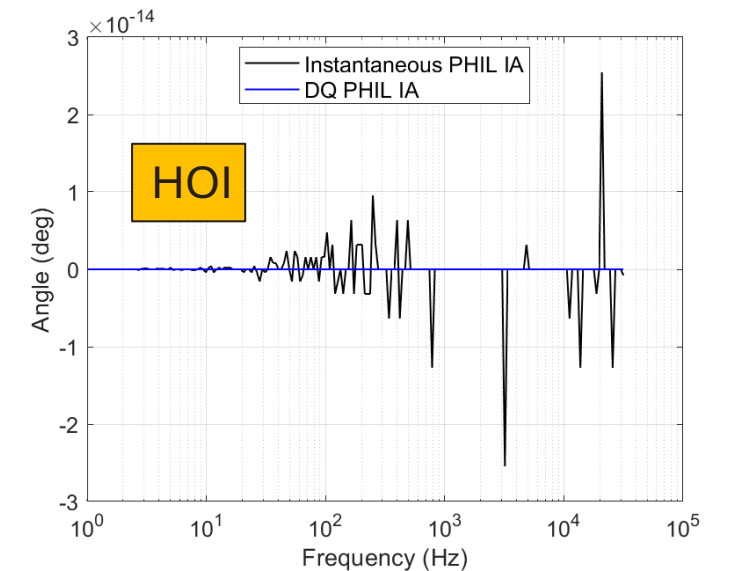
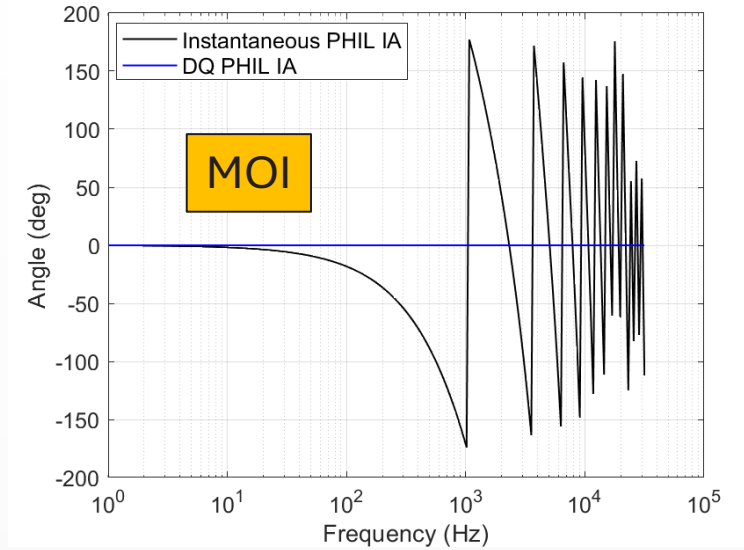
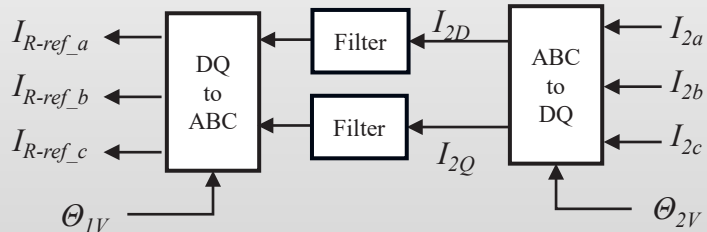


'DQ' Transformation Implementation

Voltage
to HOI

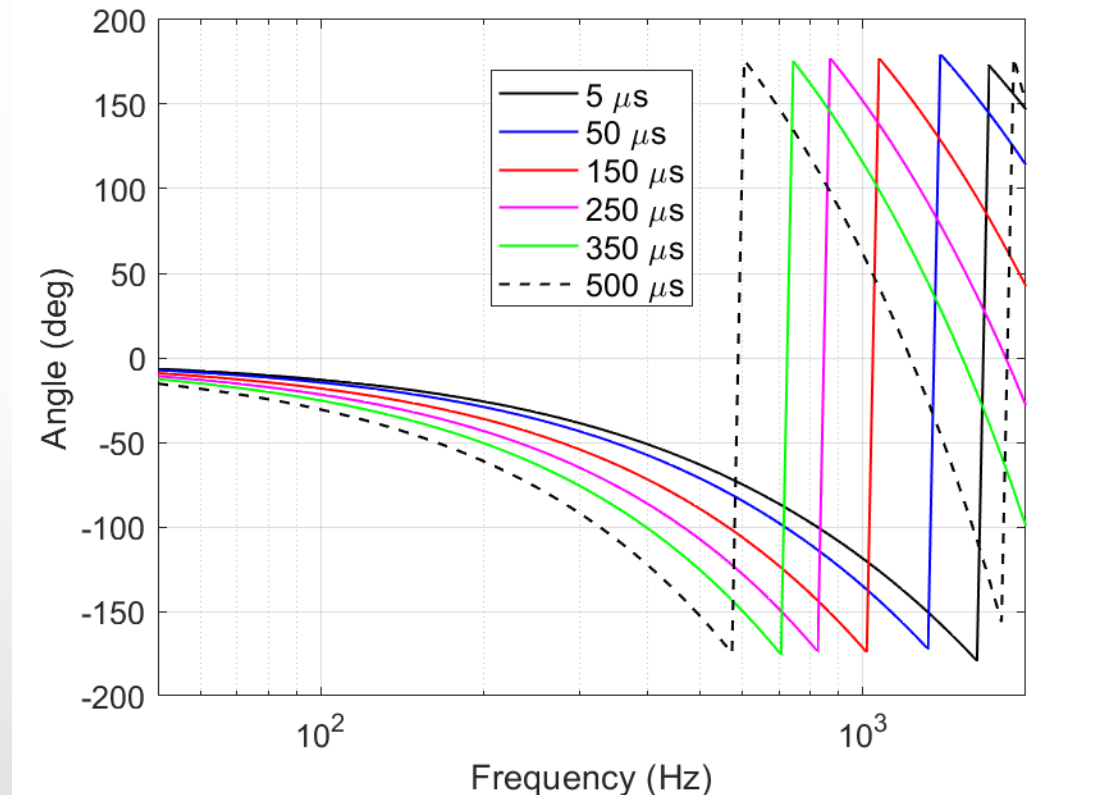


Current
to HOI



Phase Angle Accuracy Evaluation

Phase Angle at the MOI for Different Amplifier Actuation Delay



As the amplifier delay increases, the phase angle between voltage and current increases at the MOI which leads to accuracy issues with the PHIL experiment

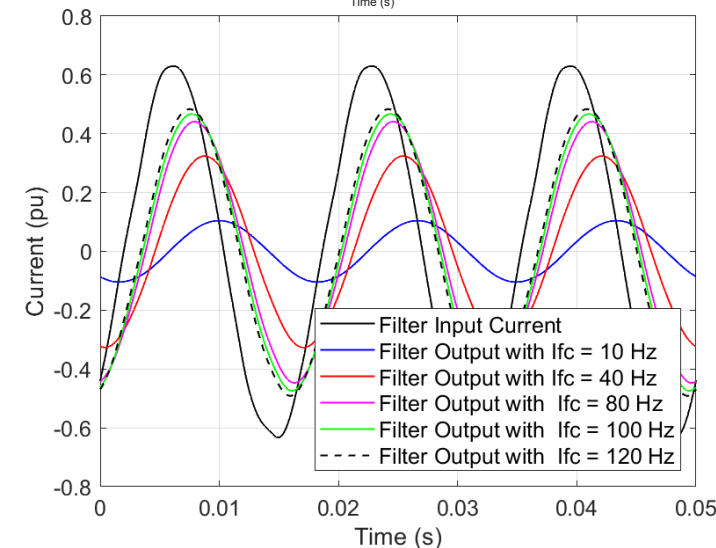
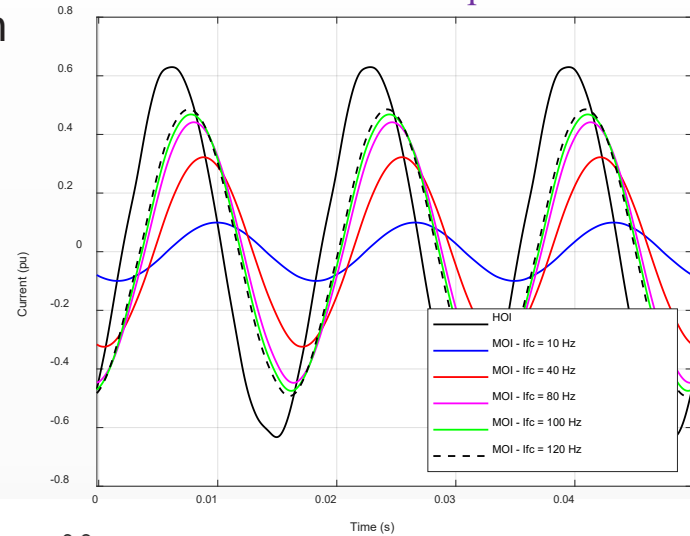
Filtering frequencies above and below fundamental

Improving Stability of PHIL Experiment

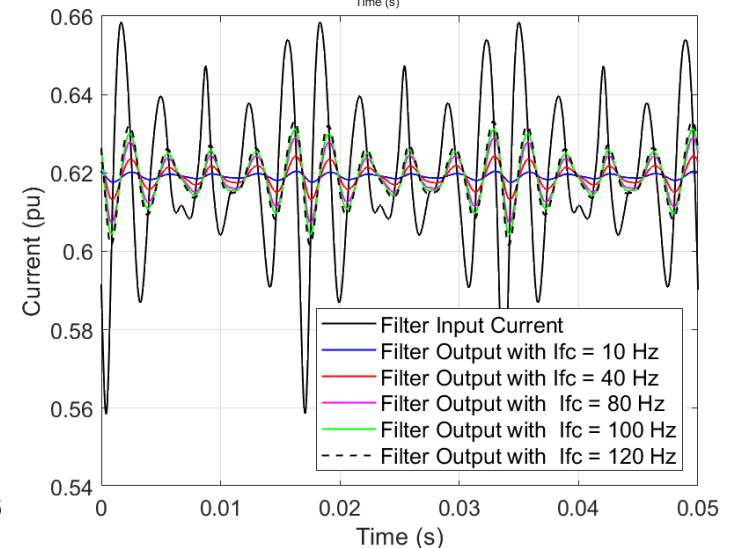
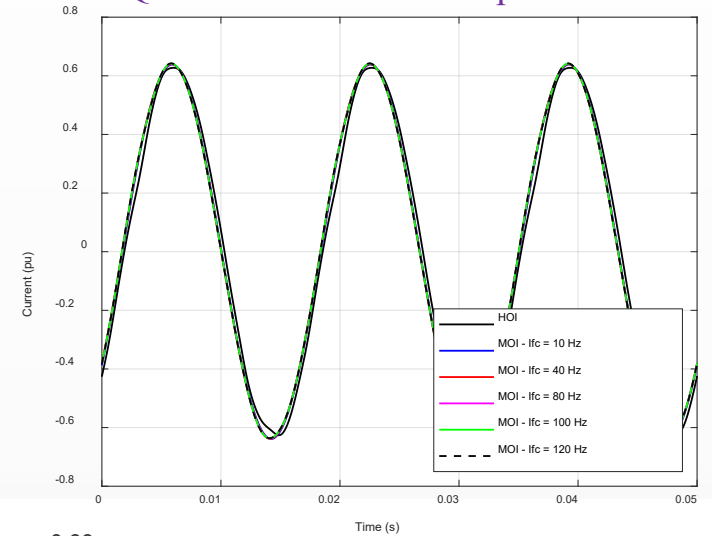
- Consider ITM-VT IA for RL benchmark system
- For certain PHIL experiments to maintain stability, filtering of the feedback current is required
- The digital side current reference I_{R-ref} is filtered using a first order filter for both 'ABC' and 'DQ' implementations
- Plots showing instantaneous waveforms for Phase A currents or voltages at either the MOI or the HOI

'DQ' transformation based IA implementation able to aid in stability as well as preserving accuracy

'ABC' Frame IA Implementation



'DQ' Transformation IA Implementation



Conclusion

- Linear analysis framework for PHIL experiments is applicable to multi-phase PHIL systems
- Although analytical expressions for stability and accuracy seem complicated, FD and TD simulations can be used for verification
- A practical example of application of linear analysis framework for three-phase PHIL experiment was demonstrated [1].

ELA Gain	Instantaneous	DQ Resistive	DQ-Resistive-Inductive
T_{1F}^*	1	$\begin{bmatrix} 1 & 0 \\ 0 & 1 \end{bmatrix}$	$\begin{bmatrix} 1 & 0 \\ 0 & 1 \end{bmatrix}$
T_{2F}^*	0	0	0
Z_{1F}^*	0	0	0
Z_{2F}^*	0	0	0
T_{1R}^*	0	0	0
T_{2R}^*	0	0	0
Z_{1R}^*	0	0	0
Z_{2R}^*	0	0	0
Z_R	$-R_R$	$-\begin{bmatrix} R_R & 0 \\ 0 & R_R \end{bmatrix}$	$-\begin{bmatrix} R_R & 0 \\ 0 & R_R \end{bmatrix}$
Z_F	Z_{Amp}	$\begin{bmatrix} R_{Amp} & 0 \\ 0 & R_{Amp} \end{bmatrix}$	$\begin{bmatrix} R_{Amp} + \omega L_{Amp} & -\omega_s L_{Amp} \\ \omega_s L_{Amp} & R_{Amp} + \omega L_{Amp} \end{bmatrix}$

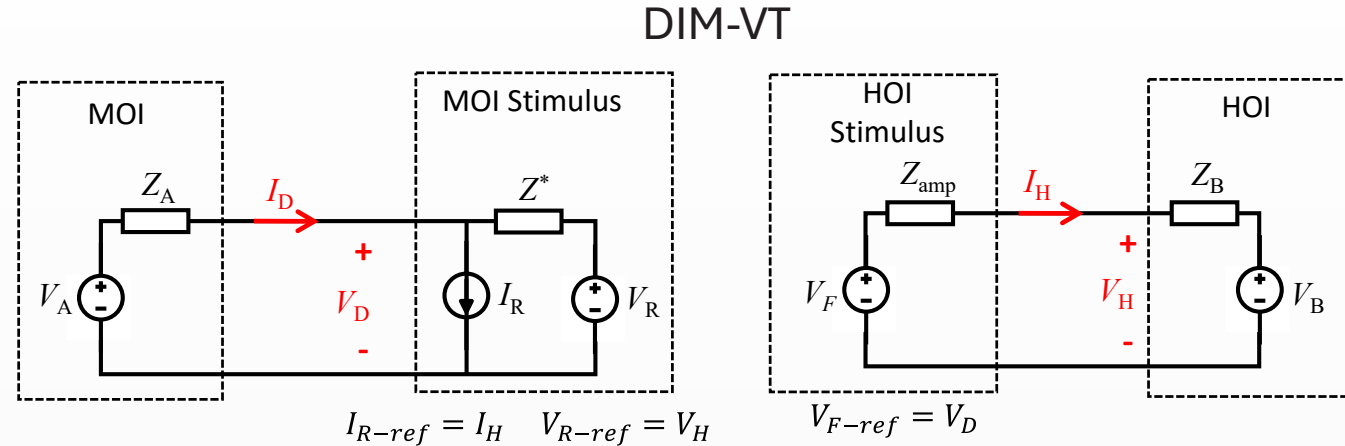
[1] S. Ishiguro, J. Langston, K. Watanabe, H. Lopez, Y. Izumida, and I. Barnola, "Using power hardware-in-the-loop simulation to explore uninterrupted power service of a converter for microgrid," in IECON 2024 - 50th Annual

Partial-Virtual DIM Interface Algorithm



Challenges with DIM IA

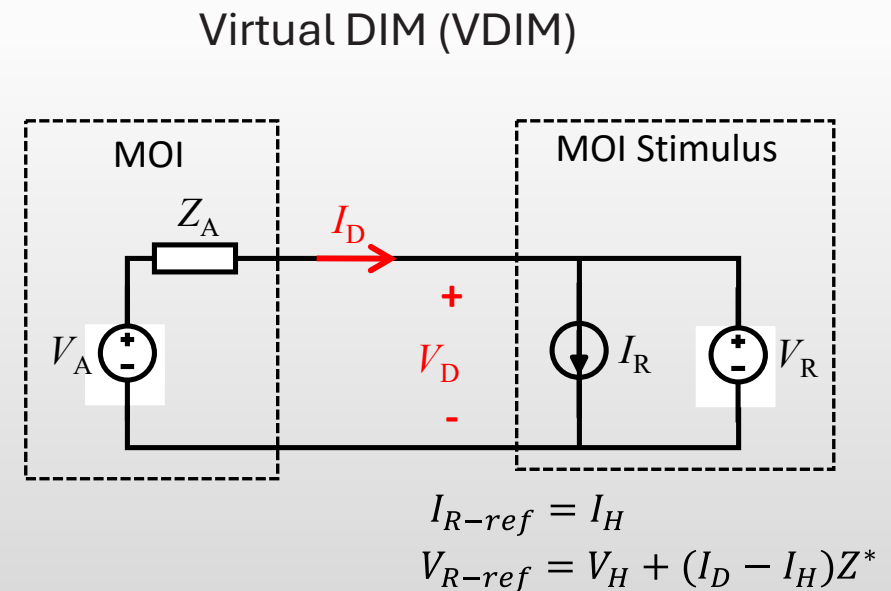
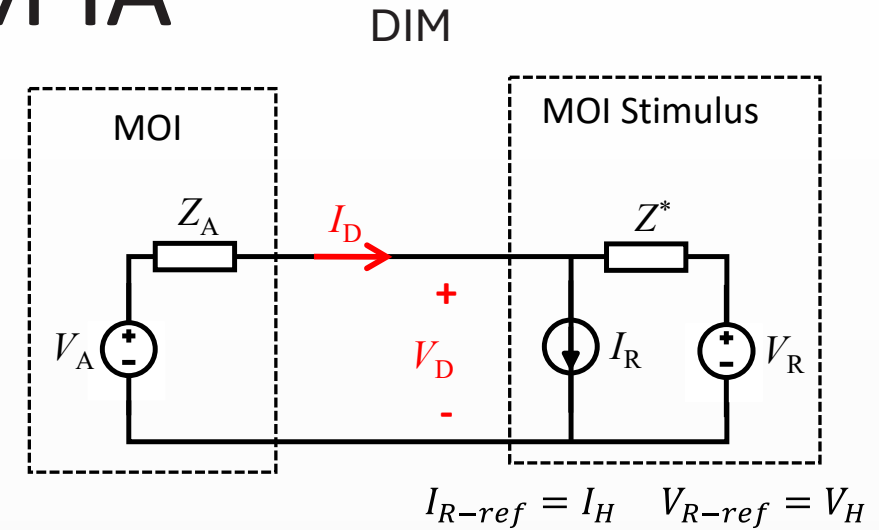
- Requires matching Z^* to Z_B over the full frequency range
- Requires measurement of Z_B
- May need to adapt Z^* to changes in Z_B
- May be difficult to represent Z_B through network of passive components
 - Controls for power electronic converters can arbitrarily shape impedance in lower frequency range
 - Constant power loads and power converters often exhibit negative resistance (i.e. 180 degree phase angle) at low frequency



Motivation for PDIM and PVDIM IAs

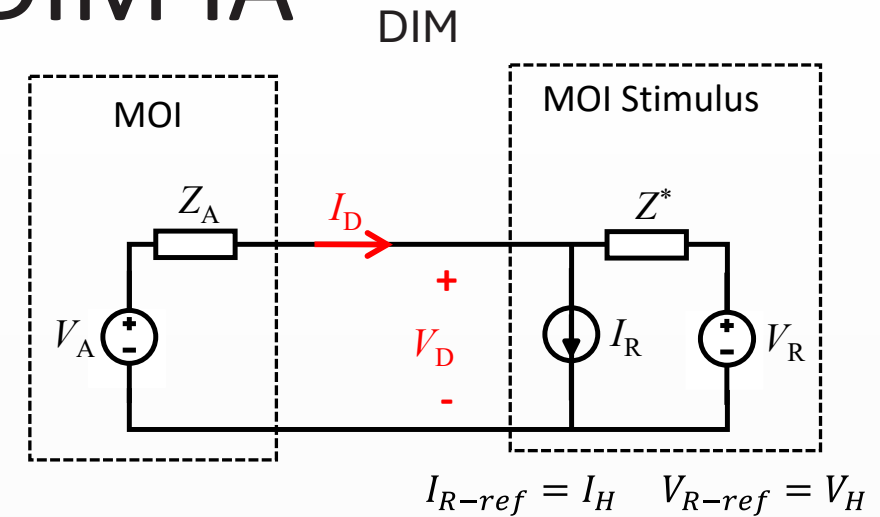
Virtual DIM IA

- Do not explicitly represent Z^* with passive elements
- Represent effect of Z^* through voltage drop
- Represent Z^* through transfer function applied to I_H
- (+) Not limited to representation as passive network
- (-) Delay in stimulus can distort the impedance at high frequency

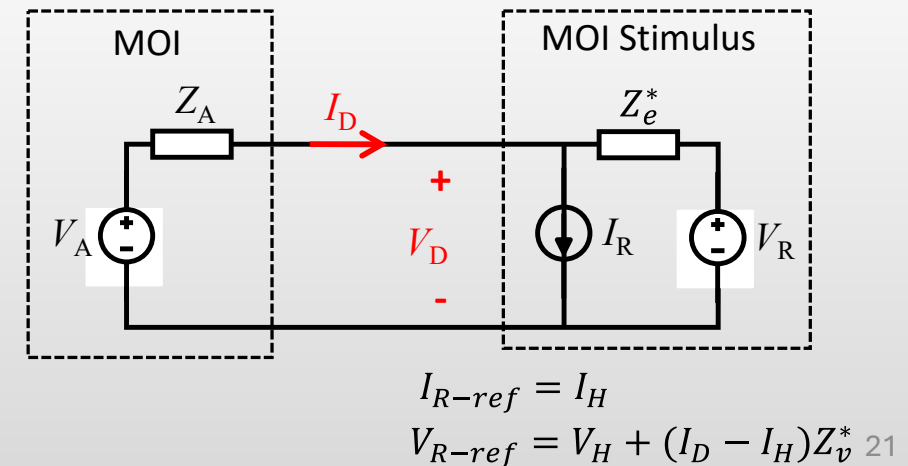


Partial Virtual DIM IA

- Represent Z^* through combination of explicit passive elements (Z_e^*) and virtual impedance (Z_v^*)
- Use Z_v^* to represent impedance in the low frequency range
 - (+) Flexibility to represent arbitrary transfer function
- Use Z_e^* to represent impedance in the high frequency range
 - (+) Avoids issues with delays in stimuli
 - (+) Typically, high frequency range is dominated by passive elements

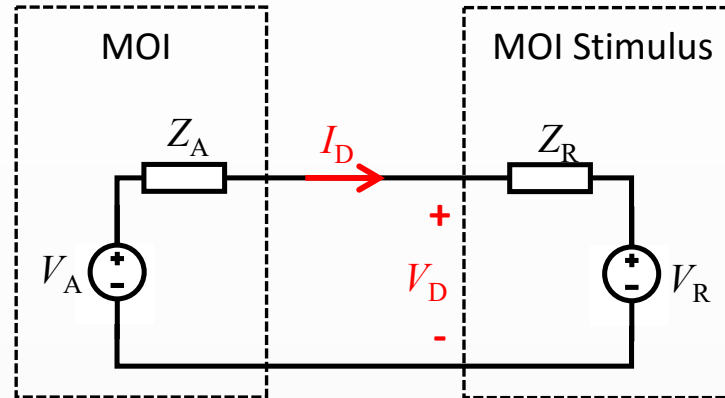


Partial Virtual DIM (PVDIM) $Z^* = Z_v^* + Z_e^*$



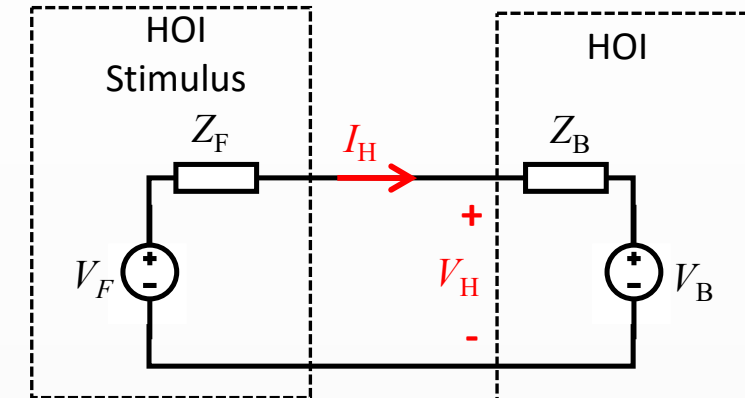
General Framework for Linear PHIL IAs

- Stimuli represented as Thevenin equivalent circuits
- Stimuli references formed from linear combination of observable quantities
- PHIL IA defined by 8 ideal “gains” and two Thevenin impedance characteristics (Z_R and Z_F)



$$V_R = T_{DR}V_D + Z_{DR}I_D + T_{HR}V_H + Z_{HR}I_H$$

$$V_{R-ref} = T_{DR}^*V_D + Z_{DR}^*I_D + T_{HR}^*V_H + Z_{HR}^*I_H$$



$$V_F = T_{DF}V_D + Z_{DF}I_D + T_{HF}V_H + Z_{HF}I_H$$

$$V_{F-ref} = T_{DF}^*V_D + Z_{DF}^*I_D + T_{HF}^*V_H + Z_{HF}^*I_H$$

PHIL IA	T_{DR}^*	Z_{DR}^*	T_{HR}^*	Z_{HR}^*	T_{DF}^*	Z_{DF}^*	T_{HF}^*	Z_{HF}^*	Z_R	Z_F
ITM-VT	0	0	0	$-Z_R$	1	0	0	0	Z_R	Z_{amp}
DIM-VT	0	0	1	$-Z^*$	1	0	0	0	Z^*	Z_{amp}
VDIM-VT	0	Z^*	1	$-Z^*$	1	0	0	0	0	Z_{amp}
PVDIM-VT	0	Z_v^*	1	$-Z^*$	1	0	0	0	Z_e^*	Z_{amp}

Example PHIL System

- Large source impedance to present stability challenge
- Negative resistance in series with parallel RLC for HOI impedance
- Delays

Symbol	Description	Value
f_{base}	Base frequency for the system.	50 Hz
f_{c-amp}	Pole frequency for filter representing the amplifier dynamics.	400 Hz
f_{c-mI}	Pole frequency for filter representing current measurement characteristics.	100 kHz
f_{c-mV}	Pole frequency for filter representing voltage measurement characteristics.	100 kHz
R_A	Source resistance.	0.05 pu
R_{amp}	Amplifier resistance.	0.005 pu
R_B	HOI impedance magnitude at low frequency.	1.0 pu
R_{dB}	HOI resistance for RLC circuit.	10.0 pu
T_{d-amp}	Amplifier time delay.	100 μ s
T_{d-mI}	Time delay associated with current measurements.	50 μ s
T_{d-mV}	Time delay associated with voltage measurements.	50 μ s
T_{d-stim}	Time delay associated with voltage and current injections at the simulated ROS.	50 μ s
X_A	Source reactance.	0.5 pu
X_{amp}	Amplifier reactance.	0.01 pu
X_{CB}	HOI capacitive reactance.	10.0 pu
X_{LB}	HOI inductive reactance.	0.07 pu

Delays

$$Z_A = \frac{X_A}{2\pi f_{base}} s + R_A$$

$$C_B = \frac{1}{2\pi f_{base} X_{CB}}$$

$$L_B = \frac{X_{LB}}{2\pi f_{base}}$$

$$Z_B = -R_B \frac{2\pi f_{cB}}{s + 2\pi f_{cB}} + \frac{L_B s}{L_B C_B s^2 + \frac{L_B}{R_B} s + 1}$$

$$T_{amp} = \frac{2\pi f_{c-amp}}{s + 2\pi f_{c-amp}} e^{-s T_{d-amp}}$$

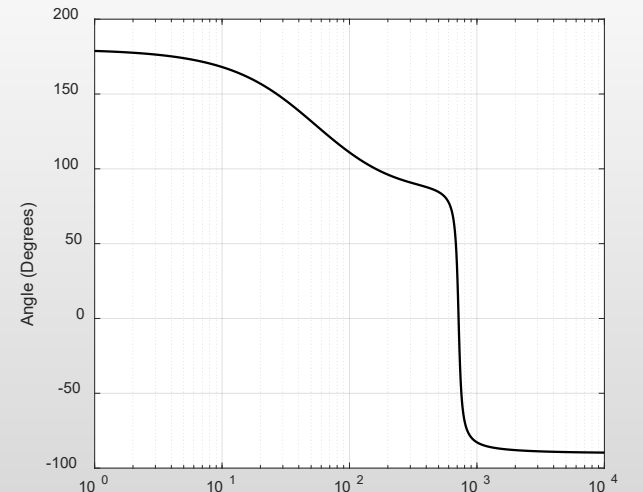
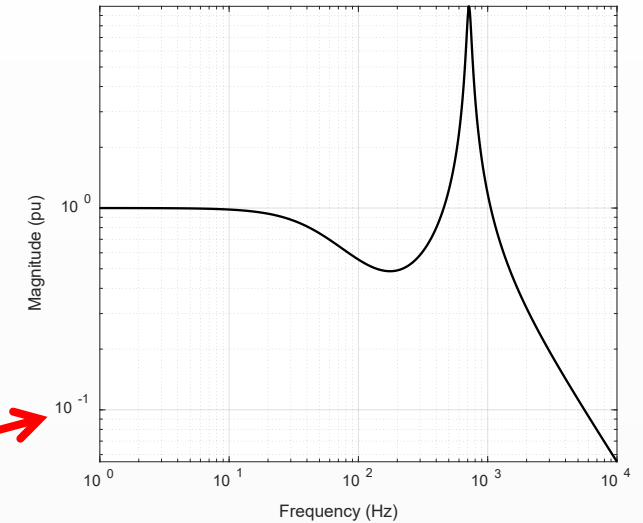
$$Z_{amp} = \frac{X_{amp}}{2\pi f_{base}} s + R_{amp}$$

$$T_{mV} = \frac{2\pi f_{c-mV}}{s + 2\pi f_{c-mV}} e^{-s T_{d-mV}}$$

$$T_{mI} = \frac{2\pi f_{c-mI}}{s + 2\pi f_{c-mI}} e^{-s T_{d-mI}}$$

$$T_{mS} = 1$$

$$T_{stim} = e^{-s T_{d-stim}}$$



Example PHIL System: IA Damping Impedance Characteristics

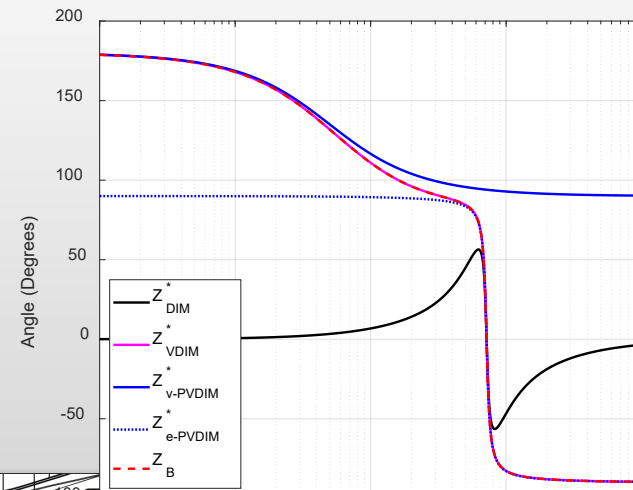
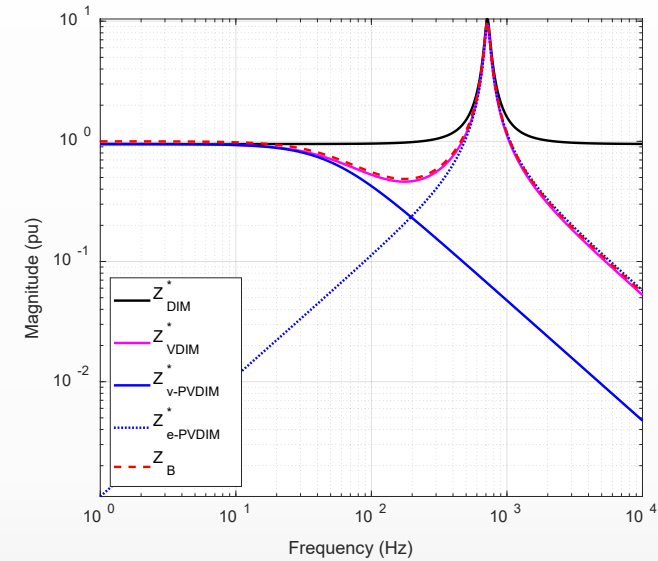
PHIL IA	T_{DR}^*	Z_{DR}^*	T_{HR}^*	Z_{HR}^*	T_{DF}^*	Z_{DF}^*	T_{HF}^*	Z_{HF}^*	Z_R	Z_F
ITM-VT	0	0	0	$-Z_R$	1	0	0	0	Z_R	Z_{amp}
DIM-VT	0	0	1	$-Z^*$	1	0	0	0	Z^*	Z_{amp}
VDIM-VT	0	Z^*	1	$-Z^*$	1	0	0	0	0	Z_{amp}
PVDIM-VT	0	Z_v^*	1	$-Z^*$	1	0	0	0	Z_e^*	Z_{amp}

$$Z_{DIM}^* = k_m R_B + \frac{k_m L_B s}{k_m^2 L_B C_B s^2 + \frac{L_B}{R_B} s + 1}$$

$$Z_{VDIM}^* = -k_m R_B \frac{2\pi f_{cB}}{s + 2\pi f_{cB}} + \frac{k_m L_B s}{k_m^2 L_B C_B s^2 + \frac{L_B}{R_B} s + 1}$$

$$Z_{v-PVDIM}^* = -k_m R_B \frac{2\pi f_{cB}}{s + 2\pi f_{cB}}$$

$$Z_{e-PVDIM}^* = \frac{k_m L_B s}{k_m^2 L_B C_B s^2 + \frac{L_B}{R_B} s + 1}$$



Linear Analysis of PHIL Experiments

Actual ELA Gains (From Ideal Gains)

$$\begin{aligned} T_{1F} &= T_{mS} T_{amp} T_{1F}^* & Z_{1F} &= T_{mS} T_{amp} Z_{1F}^* \\ T_{2F} &= T_{mV} T_{amp} T_{2F}^* & Z_{2F} &= T_{mI} T_{amp} Z_{2F}^* \\ T_{1R} &= T_{mS} T_{stim} T_{1R}^* & Z_{1R} &= T_{mS} T_{stim} Z_{1R}^* \\ T_{2R} &= T_{stim} T_{mV} T_{2R}^* & Z_{2R} &= T_{stim} T_{mI} Z_{2R}^* \end{aligned}$$

Transfer functions
describing stability,
accuracy, and sensitivity to
disturbances

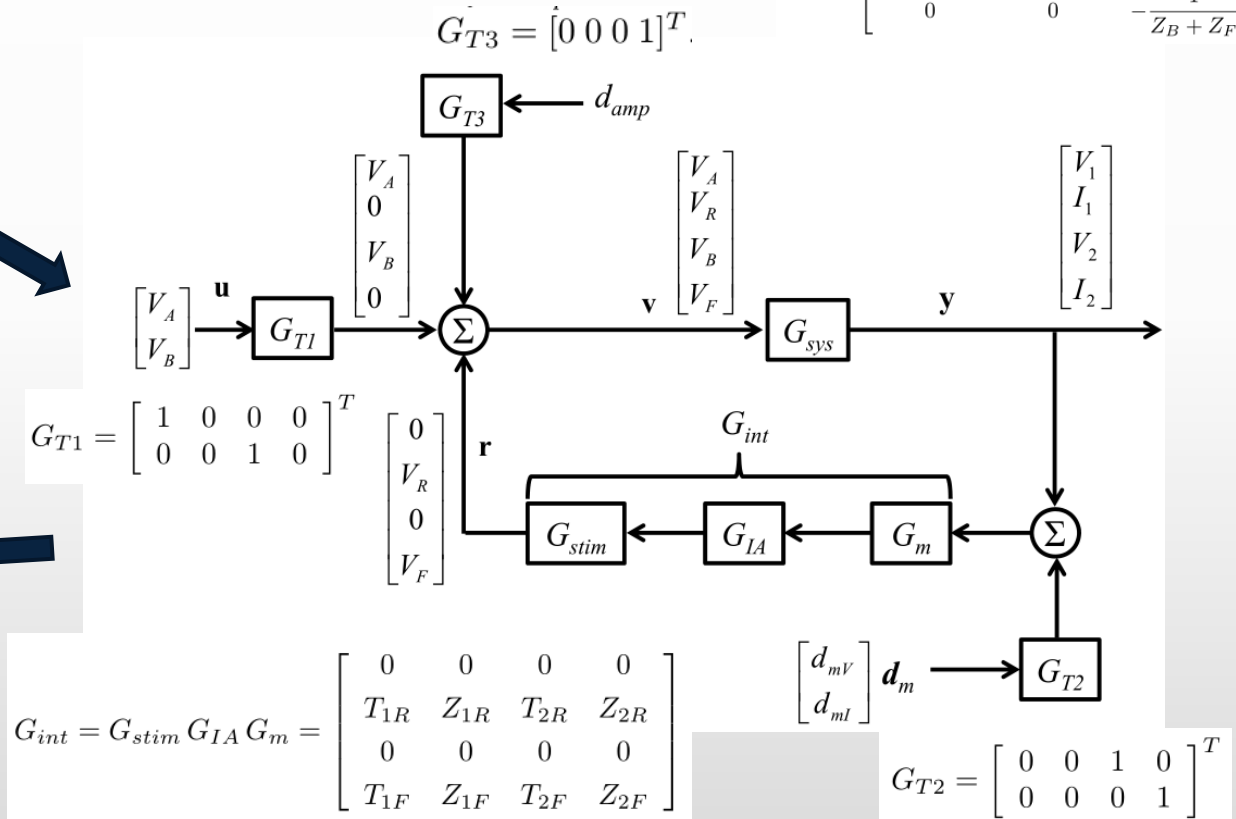
$$G_{st} = \det(I - G_{int} G_{sys}) = \det(I - G_{sys} G_{int})$$

$$T_{u-y} = (I - G_{sys} G_{int})^{-1} G_{sys} G_{T1}$$

$$T_{damp-y} = (I - G_{sys} G_{int})^{-1} G_{sys} G_{T3}$$

$$T_{dm-y} = (I - G_{sys} G_{int})^{-1} G_{sys} G_{int} G_{T2}$$

$$G_{sys} = \begin{bmatrix} \frac{Z_R}{Z_A + Z_R} & \frac{Z_A}{Z_A + Z_R} & 0 & 0 \\ \frac{1}{Z_A + Z_R} & -\frac{1}{Z_A + Z_R} & 0 & 0 \\ 0 & 0 & \frac{Z_F}{Z_B + Z_F} & \frac{Z_B}{Z_B + Z_F} \\ 0 & 0 & -\frac{1}{Z_B + Z_F} & \frac{1}{Z_B + Z_F} \end{bmatrix}$$

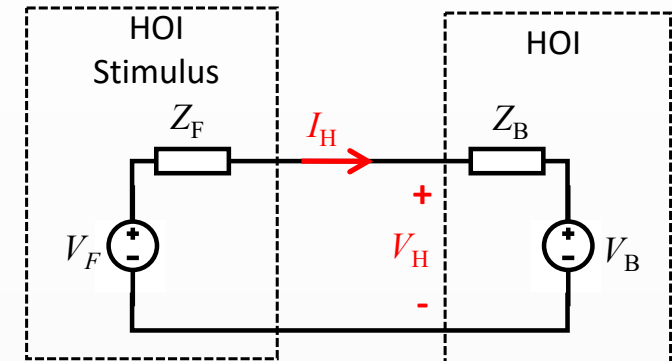
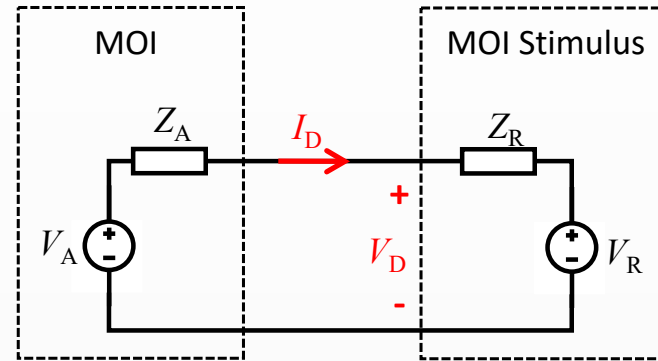


Assessment of Accuracy: Transfer Function Magnitude Error

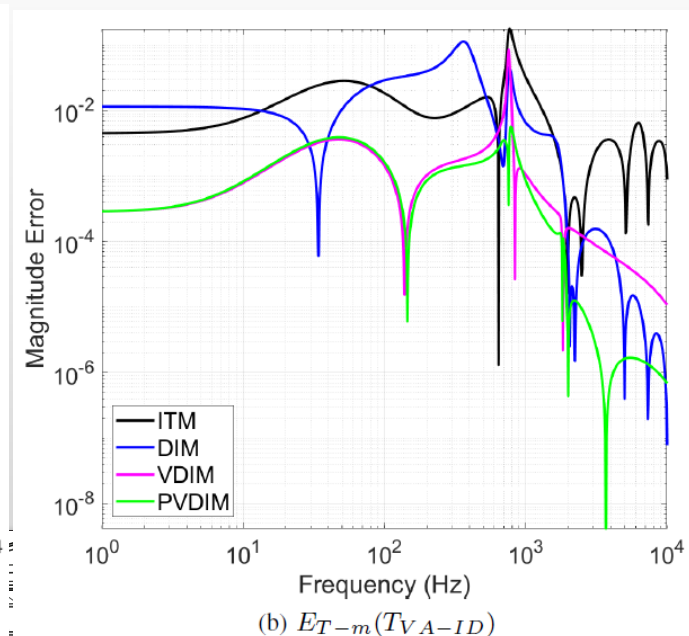
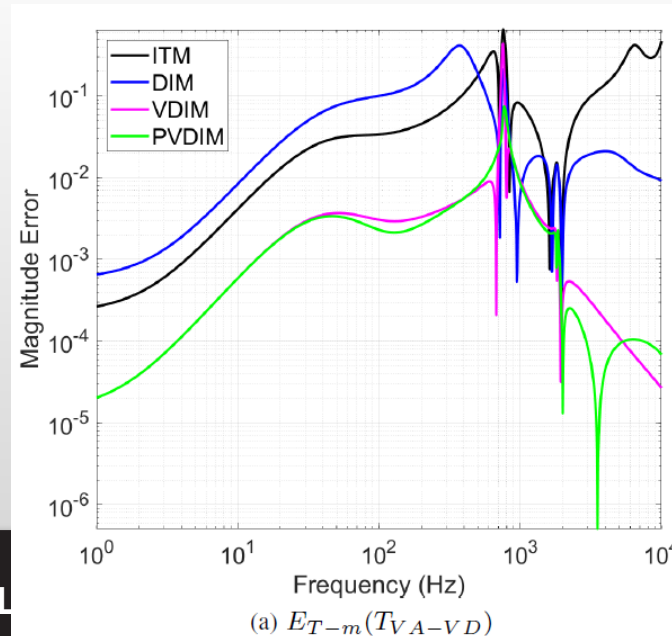
$$E_{T-m}(T) = \left| |T| - |\tilde{T}| \right|$$

$$E_{T-m}(T_{VA-VD}) = \left| \left| \frac{Z'_B}{Z_A + Z'_B} \right| - \left| \frac{Z_B}{Z_A + Z_B} \right| \right|$$

$$E_{T-m}(T_{VA-ID}) = \left| \left| \frac{1}{Z_A + Z'_B} \right| - \left| \frac{1}{Z_A + Z_B} \right| \right|$$

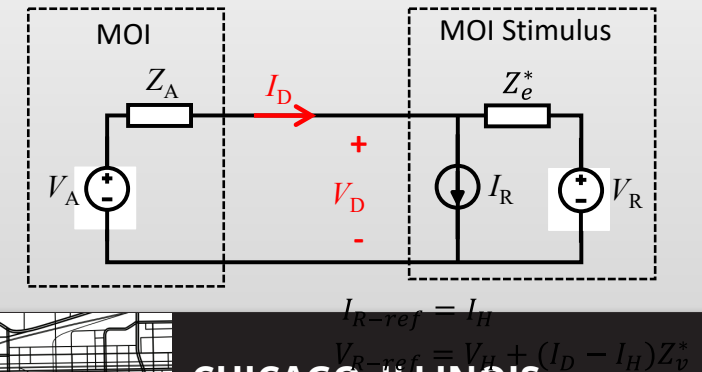
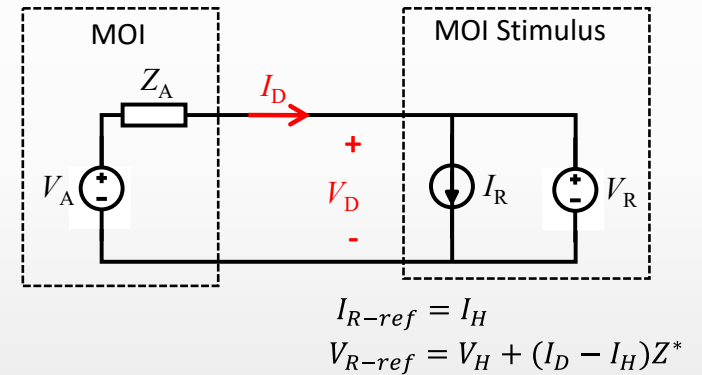
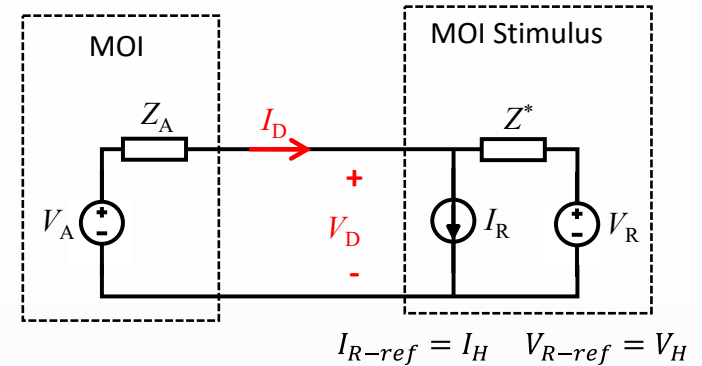


- VDIM and PVDIM generally show lower magnitude error
- PVDIM generally shows lower magnitude error in high frequency range

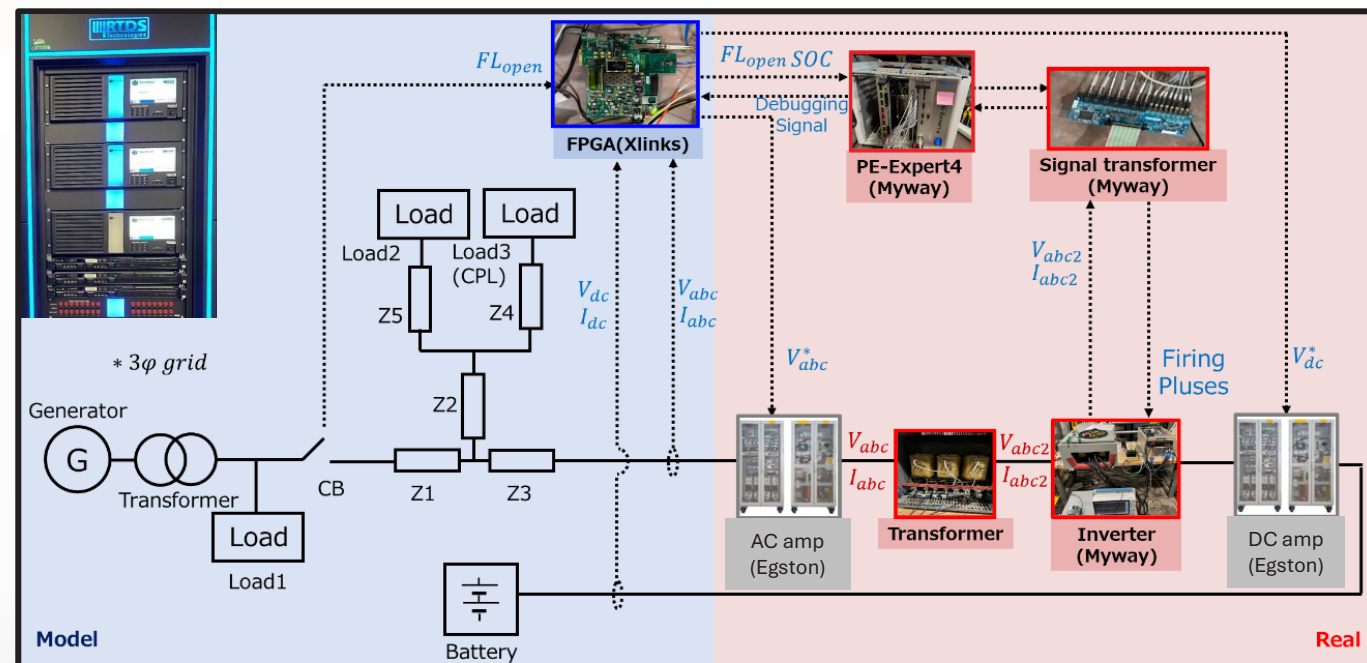


Conclusion

- DIM IA is often employed for PHIL systems posing stability challenges
- VDIM and PVDIM can offer additional flexibility in representing Z^* for the DIM IA
- Flexibility can be even more important for multi-phase PHIL IAs (e.g. DQ-frame implementations)
- PVDIM can offer improvements over VDIM if Z^* can be partitioned

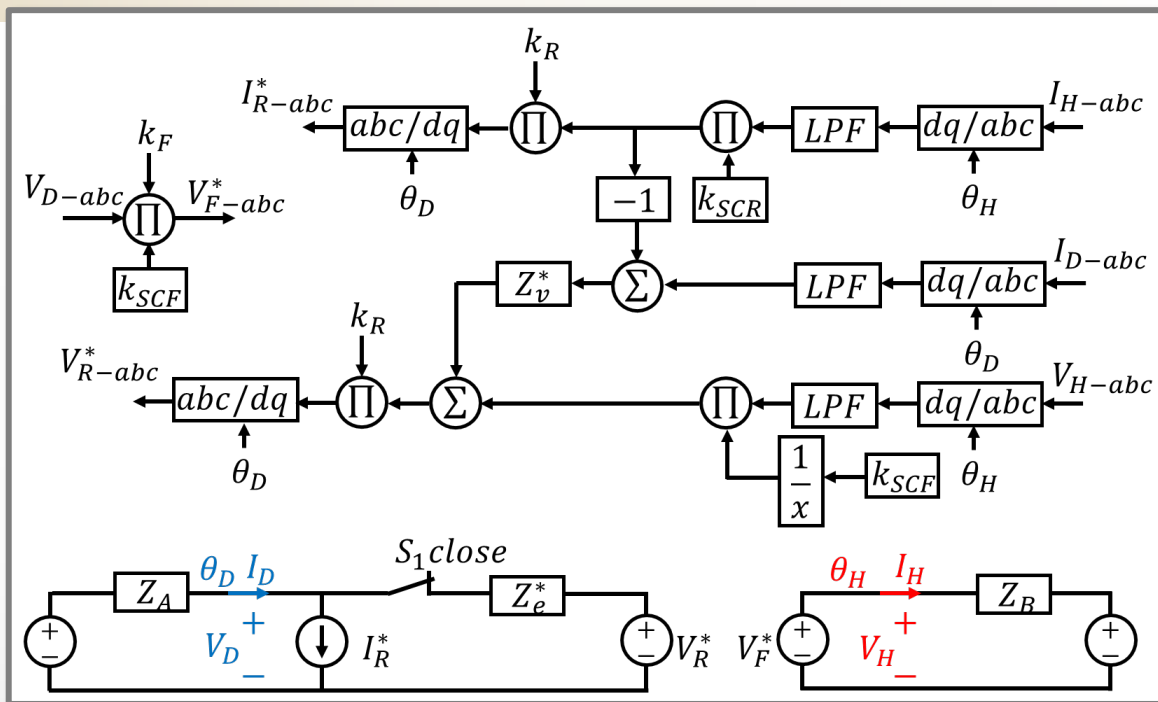


PHIL & CHIL Testing



- When DG trips, impedance rapidly switches from low impedance of DG to high impedance of loads
- Simultaneously, battery inverter switches from high impedance to low impedance

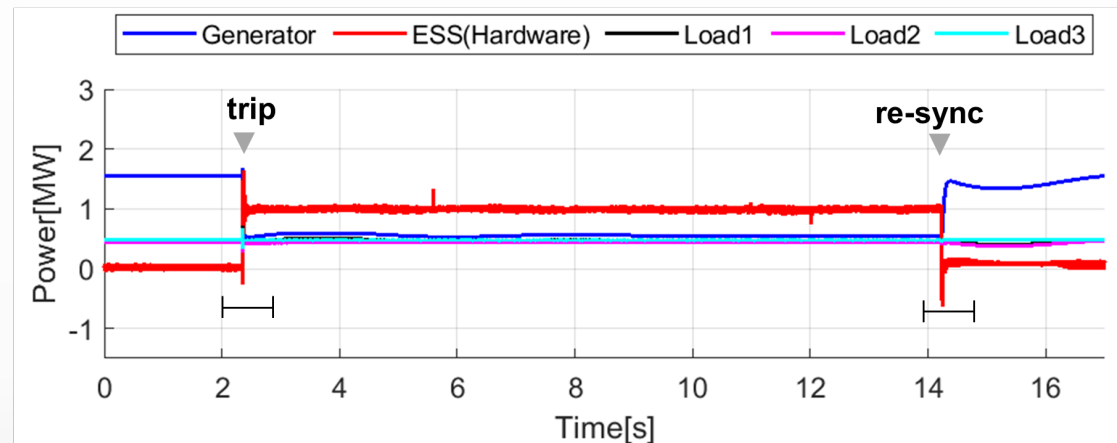
Practical Application of PVDIM



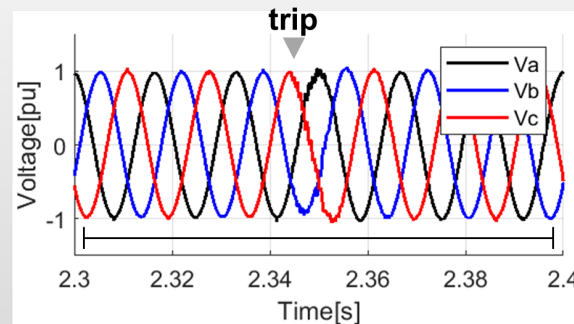
Interface Algorithm Block Diagram

ITM – VT Interface algorithm used when DG is online
PVDIM – VT Interface algorithm used when DG trips

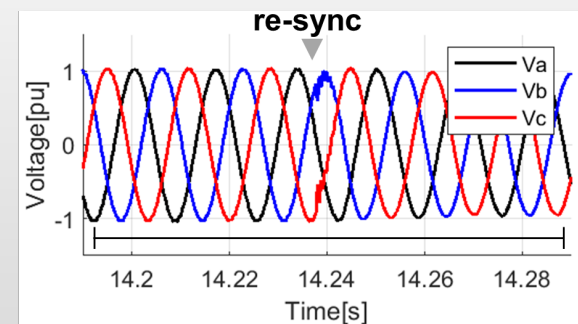
- Active power (grid-connected/islanding condition)



- Voltage wave(trip)



- Voltage wave(re-sync)



Few Publications of Interest

- J. Langston, “[Application and analysis of the extended Lawrence teleoperation architecture to power hardware-in-the-loop simulation](#),” Ph.D. dissertation, Florida State University, 2018.
- H. Ravindra, “[Linear analysis of multi-phase PHIL experiments](#),” Ph.D. dissertation, Florida State University, 2023.
- H. Ravindra and J. Langston, “[Linear Analysis of PHIL Simulation Experiments with Multi-Phase Interfaces](#),” *IECON 2024 - 50th Annual Conference of the IEEE Industrial Electronics Society*, Chicago, IL, USA, 2024.
- J. Langston, S. Ishiguro, H. Ravindra, K. Watanabe and K. Schoder, “[Partial Virtual Damping Impedance Method Interface Approach for Power Hardware-in-the-Loop Simulation](#),” *IECON 2024 - 50th Annual Conference of the IEEE Industrial Electronics Society*, Chicago, IL, USA, 2024.
- J. Langston, T. Szymanski, K. Schoder, M. Steurer, and R. G. Roberts, “[Practical estimation of accuracy in power hardware-in-the-loop simulation using impedance measurements](#),” *IEEE Transactions on Power Systems*, vol. 36, no. 3, pp. 2584–2593, 2021
- S. Ishiguro, J. Langston, K. Watanabe, H. Lopez, Y. Izumida and I. Barnola, “[Using Power Hardware-in-the-Loop Simulation to Explore Uninterrupted Power Service of a Converter for Microgrid](#),” *IECON 2024 - 50th Annual Conference of the IEEE Industrial Electronics Society*, Chicago, IL, USA, 2024.



Thank You

